Fuel Processing Technology 242 (2023) 107659

Contents lists available at ScienceDirect

Fuel Processing Technology

journal homepage: www.elsevier.com/locate/fuproc

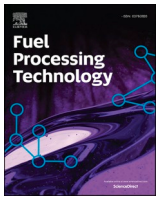

Chemistry and potential candidature of metal-organic frameworks for electrochemical energy storage devices

Teddy Mageto [a,b], Felipe M. de Souza [b], Jasvinder Kaur [d], Anuj Kumar [c,**], Ram K. Gupta [b,e,*]

[a] Department of Physics, Pittsburg State University, Pittsburg, KS 66762, USA
[b] National Institute for Materials Advancement, Pittsburg State University, Pittsburg, KS 66762, USA
[c] Nano-Technology Research Laboratory, Department of Chemistry, GLA University, Mathura, Uttar Pradesh 281406, India
[d] Department of Chemistry, School of Sciences, IFTM University, Moradabad-244102, Uttar Pradesh, India
[e] Department of Chemistry, Pittsburg State University, Pittsburg, KS 66762, USA

ARTICLE INFO

Keywords:
Metal-organic-frameworks
Flexible devices
Supercapacitors
Metal-air batteries
Metal-ion batteries
Metal-sulfur batteries

ABSTRACT

Conversion and energy storage through electrochemical devices such as batteries and supercapacitors are crucial in the establishment of sustainable energy. Metal-organic frameworks (MOFs) are a promising material to be used in these devices due to their high specific surface areas as well as tunable structures, morphology, and channel sizes. This review examines the application of MOFs in supercapacitors, Li-ion batteries, metal-S batteries, metal-O_2 batteries, and flexible electrochemical devices for energy storage with a focus on highlighting the role played by MOFs in enhancing the performance of such devices. A summary of several synthetical approaches to nanostructured MOFs is also included.

1. Introduction

1.1. Emergence of electrochemical energy storage technologies

Humanity's technological and socio-economic advancements are driven by energy. While great progress has been made in these fields, the effects of this need for energy on the environment cannot be ignored. Global warming is a major crisis facing the world today. The major contributor to this crisis is the increase in global CO_2 emissions brought about by the over-reliance on fossil fuels as a source of energy. As a result of this glaring crisis as well as the dwindling amount of fossil fuel resources, current research is focused on establishing a clean energy framework. This framework consists of two major elements: (i) renewable and clean energy matrices such as sun radiation, hydroelectric, and wind force; and (ii) devices for energy storage such as fuel cells and supercapacitors to store the generated energy. The development of these energy storage technologies has been the subject of vigorous research in recent years [1–6].

1.2. Chemistry of metal-organic frameworks

Metal-organic frameworks (MOFs) are a class of organic-inorganic materials where a metal ion and an organic ligand are coordinated to form a 3D structure. The metal ions can be alkalines, transition, or lanthanides while ligands are typically those with N- or O- donor atoms like polyamines [7]. MOF materials were first described by Yaghi et al. in 1995 [8]. MOFs attracted attention recently in the energy field. This is due to their porous structure, high specific surface area, good structural stability, active sites, and readily availability [9]; all of which make MOFs important materials for various applications ranging from drug delivery and optoelectronics to energy storage devices. MOFs also possess high tunability, where their structure, channel size, and morphology can be adjusted and controlled which provides an opportunity for the tailor-made design of MOFs for high capacitance and other specific applications [10]. When it comes to conversion and energy storage applications, MOFs can be utilized in general ways which are: (i) direct utilization; (ii) as a sacrificial material in the production of nanostructures, or (iii) as a support substrate for functional support materials such as metals and metal oxides. Utilizing MOFs as sacrificial materials is the basis of obtaining MOF-derived materials. Compared to neat MOFs and their composites, MOF-derived materials exhibit higher electronic conductivity, electrochemical performance as well as stability, as MOF-based materials tend to maintain the size, morphology, structure, and tunability of the MOF precursor through rational design

* Corresponding author at: National Institute for Materials Advancement, Pittsburg State University, Pittsburg, KS 66762, USA.
** Corresponding author.
E-mail addresses: anuj.kumar@gla.ac.in (A. Kumar), ramguptamsu@gmail.com (R.K. Gupta).

https://doi.org/10.1016/j.fuproc.2023.107659
Received 11 September 2022; Received in revised form 21 December 2022; Accepted 8 January 2023

and synthesis [11]. Additionally, there are greater possibilities in the structure and composition of porous MOF-derived materials for uses in electrochemical conversion and energy storage owing to the large amount of inorganic units and organic compounds for coordination, porosity and high surface area with rational pore-size distribution inherited from the MOF precursors [11]. The atomic composition of these MOF-derived materials can vary, and are generally grouped into several main groups including (i) Metal-free nanocarbons, (ii) transition metal/metal compound functionalized with nanocarbons, and (iii) MOF-derived composites with micro/nano-structures [12].

MOFs present great potential for use in supercapacitors [13], as the high surface area facilitates rapid mass transport of electrons thereby facilitating a greater number of electrons being released and captured. This, coupled with the high surface area and an excessive amount of active sites lead to greater specific capacitance values which are crucial for their use in the manufacture of supercapacitors. The MOFs used for this application are typically MOFs incorporated with conductive materials such as conductive polymers and carbon-based nanomaterials like graphene, as pure MOFs cannot be used in electrochemical applications owing to their low conductivity [14]. MOFs tend to be used in the manufacture of electrode materials for these supercapacitors either directly or as precursors to prepare carbon- or transition metal oxide-electrode materials [15]. Fig. 1 shows examples of mixed and pure metal oxides derived from various precursors for MOF and Fig. 2 shows a scheme for the application parameters of MOF-related materials for renewable energy. Table 1 Summarizes reviews related to MOFs for energy storage devices in comparison with the present review.

This review discusses MOF's functions in electrochemical conversion and energy storage devices. We begin with an overview of different synthesis methods employed in the synthesis of MOF nanostructures, after which we examine the various applications of MOFs in devices for energy storage, specifically: supercapacitors, batteries along with flexible electrochemical energy storage devices. These applications were the subject of previous reviews and as such, this review is also focused on the role performed by MOFs in these devices and how they improve the device performance. Through this review article, we seek to (i) provide a profound understanding of materials used to obtain MOFs, (ii) provide a summary of the most updated work on materials for the synthesis of MOFs that are suitable for supercapacitors and batteries, and (iii) showcase the essential strategies for preparing MOFs as electroactive components for supercapacitors and batteries that can optimize the performance of these devices.

2. Synthesis strategies for MOFs-based nanoarchitectures

MOFs can be synthesized via several different methods as illustrated in the timeline shown in Fig. 3. Regardless of the particular synthesis method, the MOF synthesis process is generally comprised of two steps: (i) development and fabrication of precursors for MOF such as neat MOFs and its composites; and (ii) deliberate post-treatment [20]. Pristine MOFs are obtained via the utilization of a feasible metal ion source, organic ligand, and solvent whereas MOF composites can be fabricated via several different methods namely: electrodeposition, electrospinning, embedment with a guest component, mechanical mixing, blending, and surface decoration [20]. The post-treatment step is crucial in the synthesis of MOFs as it determines the structure, morphology, and atomic composition of the final MOF-based material, which in turn determines its application [20]. For this review, we focus on the solvothermal, hydrothermal, sonochemical, mechanochemical, microwave, and electrochemical synthesis methods.

The solvothermal approach is the most used method for the synthesis of MOFs. It involves the mixing of solutions containing solvents such as acetone, diethyl formamide, dimethylformamide methanol, ethanol, and acetonitrile, to name but a few suitable inorganic salts and an organic ligand. The solution is then sealed in a closed vessel, typically an autoclave reactor, and heated above the solvent's boiling point to crystallize the dissolved material [21,22]. Fig. 4 shows a schematic of this synthesis method as applied in the synthesis of a copper-based MOF by Gupta et al. to be used in high-performance supercapacitors [23]. It should be noted that when the solvent used is water, however, the

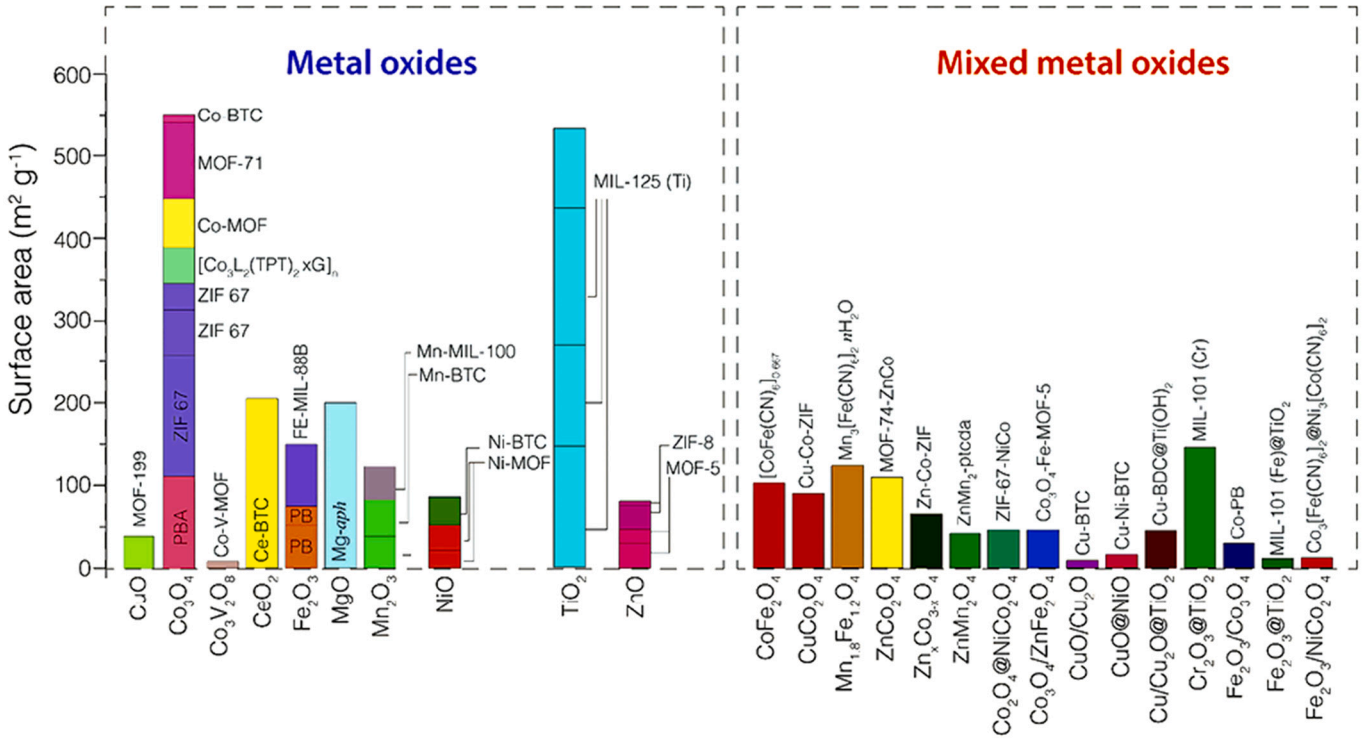

Fig. 1. Bar graphs showing the development of metal oxides used for the synthesis of MOF and mixed metal oxides and their corresponding surface area values. Adapted with permission from [13]. Copyright (2017), American Chemical Society.

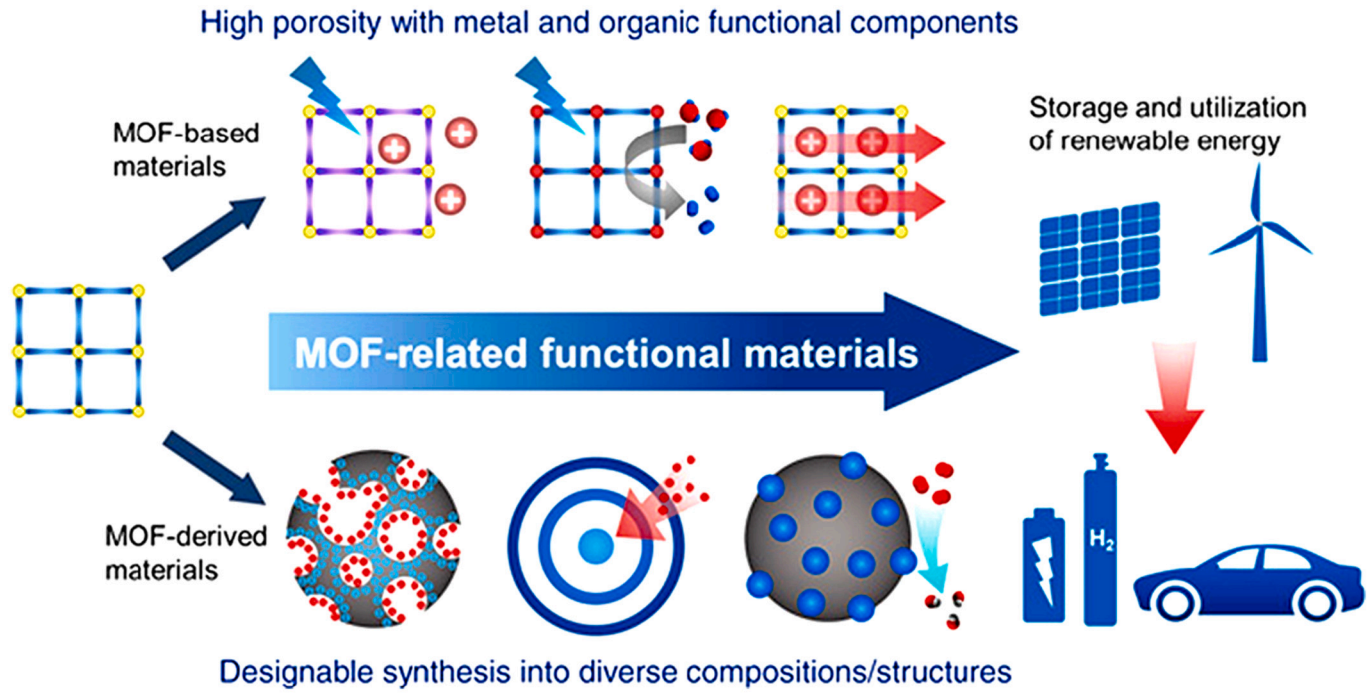

Fig. 2. Schematic of the application of MOF-related materials for renewable energy by tuning constituent components to realize different functionalities. Adapted from reference [19]. The article is distributed under a creative commons Attribution-non-commercial license 4.0 (CC BY-NC).

method ceases to be referred to as 'solvothermal' and is instead referred to as 'hydrothermal'. The hydrothermal and solvothermal synthesis processes are facile and can yield a variety of MOF samples due to the tunability of the reaction parameters such as nucleation and crystal growth rates [21]. These methods typically take from a couple of hours and can last up to days, and as such alternative synthesis methods have been developed not only to shorten reaction time but also to produce controllable nanoscale MOF crystals [24]. The rest of the MOF synthesis methods are examples of these alternate synthesis routes. The sonochemical synthesis method involves the application of ultrasound power, which is superior to other conventional sources of energy (such as electrical heating and microwaves) in terms of simplicity, efficiency, and reduced reaction time [25]. The sonochemical method has its foundation in the effect of acoustic activation, whereby bubbles are grown and collapsed sequentially at a hot spot which typically has pressures and temperatures of 1000 atm and 5000 °C respectively. Also, at cooling and heating cycles that were higher than 10^{10} K/s [25]. This effect, coupled with the application of ultrasound-induced mechanical vibrations with frequencies ranging from 20 kHz and 1 MHz, is what facilitates the rapid reaction time exhibited by this synthesis method, while also enabling the synthesis to occur at 25 °C. However, it is very difficult to control the temperature in ultrasonic baths, as they tend to heat up during use thereby resulting in uneven temperature distribution. This is thus a disadvantage to this synthesis method as sonochemical reactions often must be carried out at specific temperatures.

Mechanochemical synthesis is another alternative method used to obtain MOFs. The mechanochemical approach is based on chemical reactions which occur due to either grinding or milling in absence of or with minimal amounts of solvent [26]. This is important when it comes to obtaining MOFs as synthesis via the solvothermal approach has the disadvantage of solvent molecules remaining within the MOF framework, with solvent removal processes leading to the collapse of the said framework [27]. Effective solvent removal processes are quite costly thus mechanochemical synthesis process comes into the picture as a way to eliminate the need for solvent removal by making the MOF synthesis process solvent-free. Mechanochemical synthesis also has the added advantage of producing ample amounts of pure MOF material to be applied in a wide range of testing that can be more advantageous when analyzed against other common synthesis methods [27]. However, the end products of the mechanochemical approach are subject to contamination from milling balls, grinding containers, or the by-product phase [28].

Microwave-assisted synthesis involves the generation of microwave radiation from a magnetron that interacts with polar molecules of the solvent or substrate, converting the microwave radiation into heat via collisions between the molecules that rotate as a result of the oscillating electric field [29]. This heating is rapid and thus facilitates faster reaction times when compared to other synthesis methods. Additional advantages of employing the use of microwave-assisted synthesis include morphology control due to controlled and rapid cooling, low energy consumption, and high efficiency [29]. Furthermore, particle size and composition tend to be more uniform, and the MOFs fabricated display more satisfactory thermal stability compared to MOFs fabricated through hydrothermal synthesis along with condensation reflux as Chen et al. demonstrated in their study on nickel-based MOF-74 fabrication [30].

Finally, electrochemical synthesis in a general sense involves the use of electrical energy to direct chemical change. Electrochemical synthesis is mainly employed to generate and deposit thin films of a MOF-based material on a given substrate. These MOF-based films can be straightly deposited through processes such as anodic dissolution or indirectly through processes such as galvanic displacement and self-templated synthesis [31]. Anodic dissolution is the most well-known and broadly used electrochemical synthesis approach. It involves the oxidation of the metal source into metal ions in a solution that contains the electrolyte along with the organic ligand via the application of electric potential at the anode, after which the ions react with the ligand and form the MOF thin film on the electrode [31]. Rapid synthesis and tunable thickness are the essential advantages for electrochemical synthesis over other approaches; however, this synthetical method is not suitable for manufacturing MOF thin films as it requires high voltage and current requirements.

Table 1
Summary of reviews related to MOFs for electrochemical energy storage devices compared with the present review.

Title	Focus	Ref.
Chemistry and potential candidature of MOFs for electrochemical devices for energy storage.	Herein we emphasize the role played by MOFs and materials used to synthesize MOFs in improving the electrochemical performance of devices for energy storage. The synthesis methods of these materials and their applications across distinct devices for energy storage are also summarized.	This work
Freestanding metal–organic frameworks and their derivatives: An emerging platform for electrochemical energy storage and conversion.	Focuses on the latest advances in property-structure and synthetical approaches of freestanding electrodes for electrochemical energy storage devices that are either MOF-based or MOF-derived and the current challenges faced in their development.	[16]
Recent electrochemical applications of metal-organic framework-based materials.	Describes the application advances of MOFs and their composites for electrochemical sensors, energy storage devices, and electrocatalysis.	[17]
Metal-organic framework-derived nanoporous metal oxides toward supercapacitor applications: Progress and prospects.	Summarizes the recent advancements related to metal oxide nanomaterials and nanocomposites used for the synthesis of MOF-based components. Along with that, it addresses the recent issues and the tendency in the application of these materials for supercapacitors.	[13]
Metal-organic framework-based materials for energy conversion and storage.	Discussion on the engineering principles of tailoring the nanostructure and selecting the proper components for the synthesis of neat MOFs, its composites, and MOF-derived materials used in electrochemical energy conversion and storage applications.	[18]

3. Advancements in MOFs-based materials for electrochemical energy storage devices

3.1. MOFs-based materials for supercapacitors

Supercapacitors have attracted the attention as promising materials suitable for energy storage applications in recent years due to their effective rate of charge and discharge, appreciable stability over long electrochemical cycles, capability to deliver a large amount of energy over a short time, and comparatively low costs [32]. Supercapacitors have recently found applications in electric vehicles, utilities, energy, medical fields, and aerospace, among others [33]. There are three main types of supercapacitors: electrical double-layer capacitors (EDLC), pseudo, and hybrid supercapacitors (HSC). Fig. 5 presents the schematic representations of these supercapacitors. In general, supercapacitors store energy based on the adsorption/desorption of ions in an electrolyte.

Energy in EDLC is stored based on charge separation between the electrode and electrolyte, which is a non-Faradaic process. This interface is referred to as an electric double layer or as Helmholtz double layer, formed when an electric potential is placed across the supercapacitor electrodes that leads to charge accumulation at the electrode's surface [35]. While EDLCs show rapid charging and discharging rate and appreciable stability as a consequence of the absence of Faradaic redox reactions, they also exhibit low energy densities and low amounts of charges that can be physically stored in the device [14]. Pseudocapacitors utilize reversible Faradaic redox reactions in their charge storage mechanism, whereby reduction and oxidation occur on the electroactive material, and charges pass across the double layer thereby generating Faradaic current in the pseudocapacitor [35]. When in comparison to EDLCs, the pseudocapacitors show considerably higher energy density values but also exhibit low power densities and, because of the presence of Faradaic redox reactions, lower cycle stabilities. Hybrid supercapacitors contain both EDLC and pseudocapacitor mechanisms, thereby seeking to take advantage of the large specific capacitance and high energy densities of pseudocapacitors while also providing good cycle stabilities and high power densities present in EDLCs [35]. In general, MOFs are utilized in supercapacitors mainly as electrode materials. This is applied in one of two ways: (i) MOFs are directly utilized as electrode materials, or (ii) MOFs are utilized as templates for the fabrication of metal oxides, metal phosphides, metal sulfides, and porous carbons which are then used as electrode materials. The rest of this section will illustrate how MOFs have been used in supercapacitors, with Table 2 summarizing the main findings from these MOF applications.

Wang et al. fabricated Bi-MOF-derived Bi_2O_3/C nanofibers and NiCo-MOF-derived $NiCo_2S_4$ nanofibers which are suitable as electroactive components in asymmetric supercapacitors (ASC) [36]. The synthesized nanofibers are hollow and tubular; and because of being MOF-derived, possess a porous core-shell structure. This leads to a larger active surface area, enhanced conductivity, and improved ionic transportation. The result of these improvements is excellent electrochemical performance, as is evidenced by the results obtained by the researchers when the synthesized $NiCo_2S_4$ nanofibers and Bi_2O_3/C nanofibers were

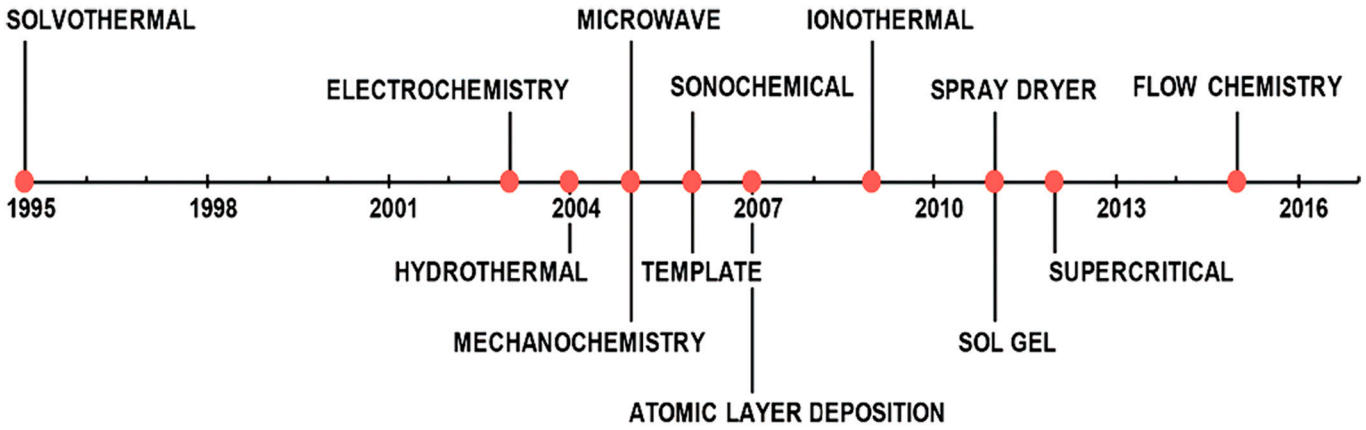

Fig. 3. Timeline showing patented synthesis approaches for the synthesis of MOFs. Adapted with permission [11]. Copyright (2017), The Royal Society of Chemistry.

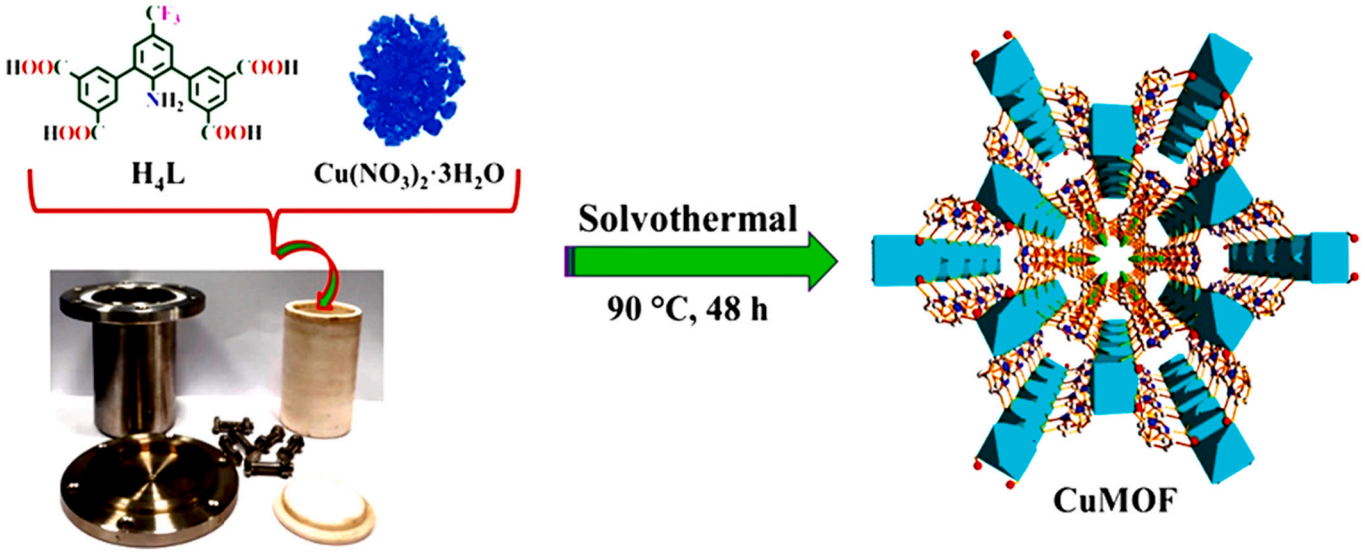

Fig. 4. Schematic of the solvothermal synthesis method as applied to the synthesis of CuMOF. Adapted with permission [23]. Copyright (2019), American Chemical Society.

employed as cathode and anode materials, respectively in an assembled ASC device. The device's energy density was 85.38 Wh/kg while displaying 80% retention after 10,000 cycles which showed an excellent performance. Another example of utilizing MOF-derived materials as electrode materials is observed in a study by Li et al. in which a ZIF-67-derived CoC_x/carbon composite array was synthesized via carbonization of a ZIF-67/Co array and used as a cathode material in an ASC device [37]. Carbonization of MOF materials is a common practice employed by researchers to preserve both porous MOF structure and the high surface area of the MOF material. In addition to this, carbonization tends to improve MOF conductivity which is crucial for electrochemical applications. The as-synthesized CoC_x/carbon composite arrays in this study exhibited high power as well as high energy densities along with excellent rate capability [37] because of the direct and unblocked ion transport pathways provided by the MOF-derived electrode's arrayed structure.

Xu et al. synthesized a highly enhanced NiCo-MOF material using a nitrate precursor to be applied as electrode material in asymmetric solid-state supercapacitors [38]. While monometallic MOFs have been studied in previous works, they have inherent disadvantages which include unstable structures and poor conductivity. Employing the use of a bimetallic MOF material such as NiCo-MOF overcomes these challenges. This study utilized both nitrate and chloride precursors in the synthesis of the NiCo-MOF nanosheets. Utilization of the chloride precursor lead to the synthesized MOF exhibiting a stacked nanosheet structure which was found to be a hindrance to ion exchange during electrochemical applications. The application of the nitrate precursor caused the resulting MOF to have a leaf-like intercalation structure with ultrathin and cross-arranged nanosheets [38]. This MOF structure facilitates rapid ion transport during electrochemical testing, resulting in excellent electrochemical performance. The assembled ASC utilizing the NiCo-MOF as a cathode material exhibited a power density of 750.89 W/kg and an energy density of 88.84 Wh/kg because of these factors.

In another example, Wang et al. obtained nanosheets of ultrathin NiCo-MOF to be applied as an electrode material for high-performance on supercapacitors [32]. It is known that MOFs exhibit a non-negligible electric resistance and relatively low electrochemical stability, which limits their application in supercapacitors. One of the ways to resolve this issue is to develop and synthesize layer-structured MOFs. Therefore the MOFs fabricated in this study were of the nanosheet morphology. The nanosheets NiCo-MOF were synthesized through an ultrasonication process at room temperature based on an adapted Tang's method. A simple schematic showing this synthesis process is seen in Fig. 6a. From the CV plots in Fig. 6b, the synthesized NiCo-MOF-based electrode is observed to have the largest CV area and as such suggests that a higher specific capacitance is a result of the synergistic effect of the Co and Ni ions. The pseudocapacitive behavior of the NiCo-MOF electroactive material is further confirmed by the non-linearity of GCD curves in Fig. 6d and e. The results presented in the study showed a specific capacitance of around 1202.1 F/g at 1 A/g as can be observed in Fig. 6f, which is higher than those of Co-MOF and Ni-MOF at the same conditions of current density. This trend was kept even as higher current densities. This MOF was then utilized as an electrode in an asymmetric supercapacitor which displayed a satisfactory electrochemical performance with energy and power densities of around 49.4 Wh/kg and 562.5 Wh/kg, respectively in a working voltage of 1.5 V. The superior electrochemical performance can be attributed to the nanosheet structure of the NiCo-MOF that facilitated the activity of more active sites for electrochemical activity while also providing a smaller channel for diffusion and electron transfer processes of the electrolyte. This can further be confirmed by the CV peaks, in which the peak currents are observed to gradually improve with an increment in scan rate with the redox peaks still being observed up to a scan rate of 70 mV/s. This is a clear indication of excellent rate performance and kinetic reversibility.

Another example of utilizing layer-structured MOFs as electrode materials are observed in the study performed by Yang et al. in which a 2D, layered, nickel-based MOF (Ni-MOF-24) was synthesized and employed as an electroactive material for high-performance supercapacitor [39]. The Ni-MOF-24 was synthesized through a feasible solvothermal approach. The study reports large specific capacitances of 1127 and 668 F/g at different rates of 0.5 and 10 A/g, respectively as shown in Fig. 7g; as well as satisfactory stability along with around 90% performance retained after 3000 cycles as displayed in Fig. 7h. These results can be attributed to the inherent feature of the fabricated Ni-MOF-24, specifically the layered structure and favorable exposed facets. The study reports that the exposed facets in particular the (100) played a major role as it was the most exposed facet. Such factors promoted the excellent transportation rate of electrons and electrolyte diffusion owing to the inherent structure of this facet. Additionally, the CV curves revealed that Ni-MOF material with more exposed facets would exhibit the best electrochemical properties as both the anodic and cathodic peaks were linearly dependent on the square of the scan rate, confirming electrolyte diffusion as the dominant phenomenon in the redox reaction for Ni-MOF. Fig. 7a shows a scheme representation of the

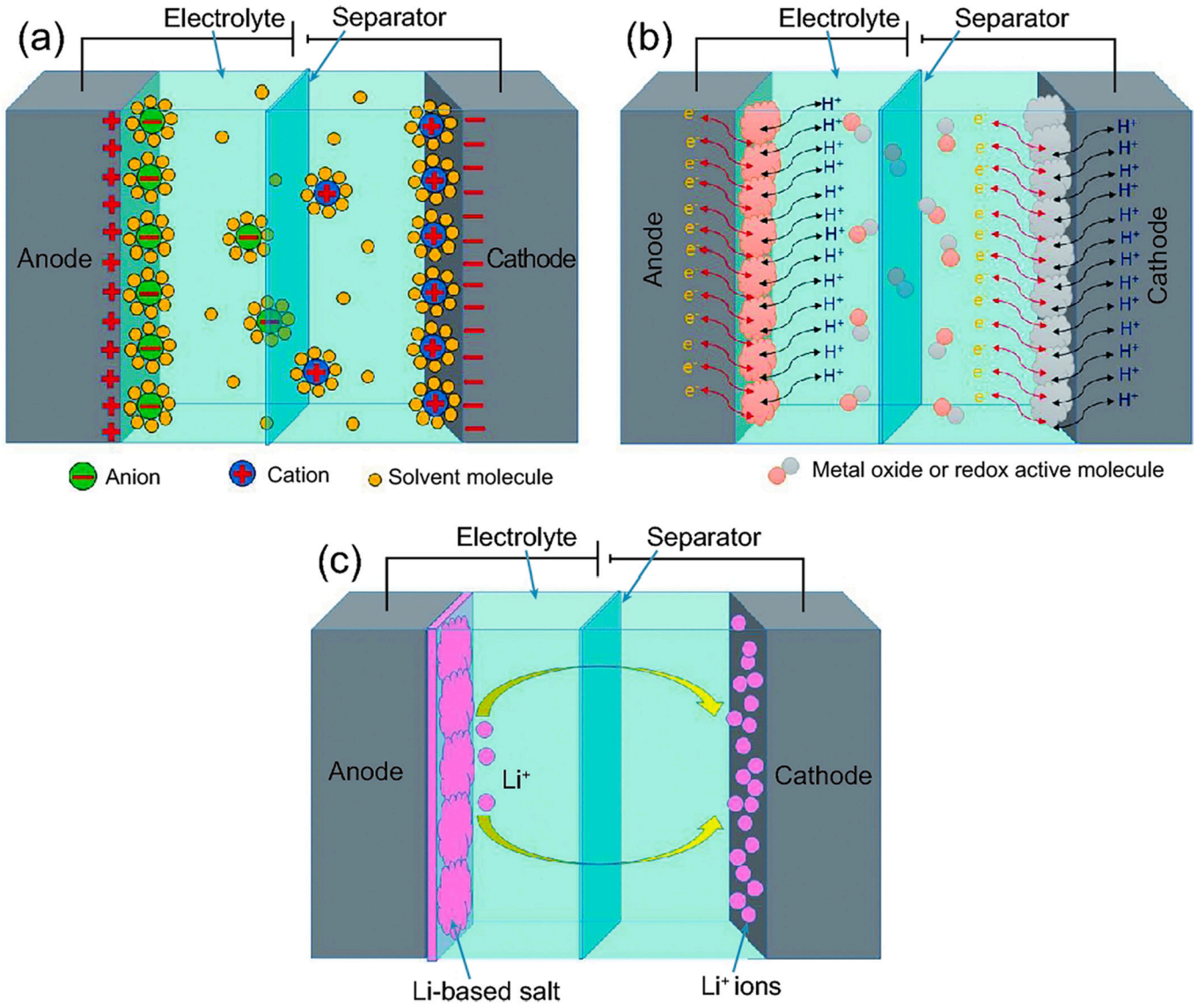

Fig. 5. Scheme for the three main types of supercapacitors: (a) EDLC, (b) pseudocapacitor, and (c) HSC. Adapted from reference [34]. The article is distributed under a Creative Commons Attribution License 4.0 (CC BY).

Table 2
Overview of MOF and materials derived from MOF along with some of their electrochemical performance values for use as supercapacitors compared with other electrocatalysts.

Material	Synthesis method	Electrolyte	Specific capacitance	Retention (%)	Reference
Bi-MOF-derived Bi_2O_3/C nanofibers	Solvothermal	2 M KOH	1420 F/g	92.21	[36]
NiCo-MOF-derived $NiCo_2S_4$ nanofibers			2656 F/g	92.11	
ZIF-67/Co	MOF-CVD	1 M KOH	338.4 F/g	95.9	[37]
NiCo-MOF	hydrothermal	2 M KOH	2860 F/g	90	[38]
NiCo-MOF	ultrasonication	2 M KOH	1202.1 F/g	89.5	[32]
Ni-MOF-24	solvothermal	6 M KOH	1127 F/g	90	[39]
Ni-MOF@GO	ultrasonication	2 M KOH	2192.4 F/g	85.1	[40]
MWCNT@Ni(TA)	solvothermal	2 M KOH	115 mAh/g	81.6	[41]
GrP/10-MnO_2	Electrochemical deposition	50 mM Na_2SO_4	385.2 F/g	85.4	[42]
ONPC	carbonization	6 M KOH	230 F/g	72	[43]

structure of the Ni-MOF-24 synthesized in this study, with Fig. 7c, d, and e showing the layered, loosely packed, sheet-like structure of the Ni-MOF-24.

Another way to resolve the issue of poor electrical conductivity in MOFs is to introduce conductive additives into the MOF such as carbon nanotubes (CNT), conductive polymers, and graphene, and employ these MOF composites as electrode materials. Zhou et al. fabricated a graphene oxide (GO) hybrid Ni-based MOF via an in-situ process shown in the schematic in Fig. 8a for pseudocapacitor applications [40].

The pseudocapacitive properties of both the Ni-MOF and the Ni-MOF/graphene oxide composite hybrid (Ni-MOF@GO) were analyzed. The CV profiles of all the synthesized MOF materials, such as the curve

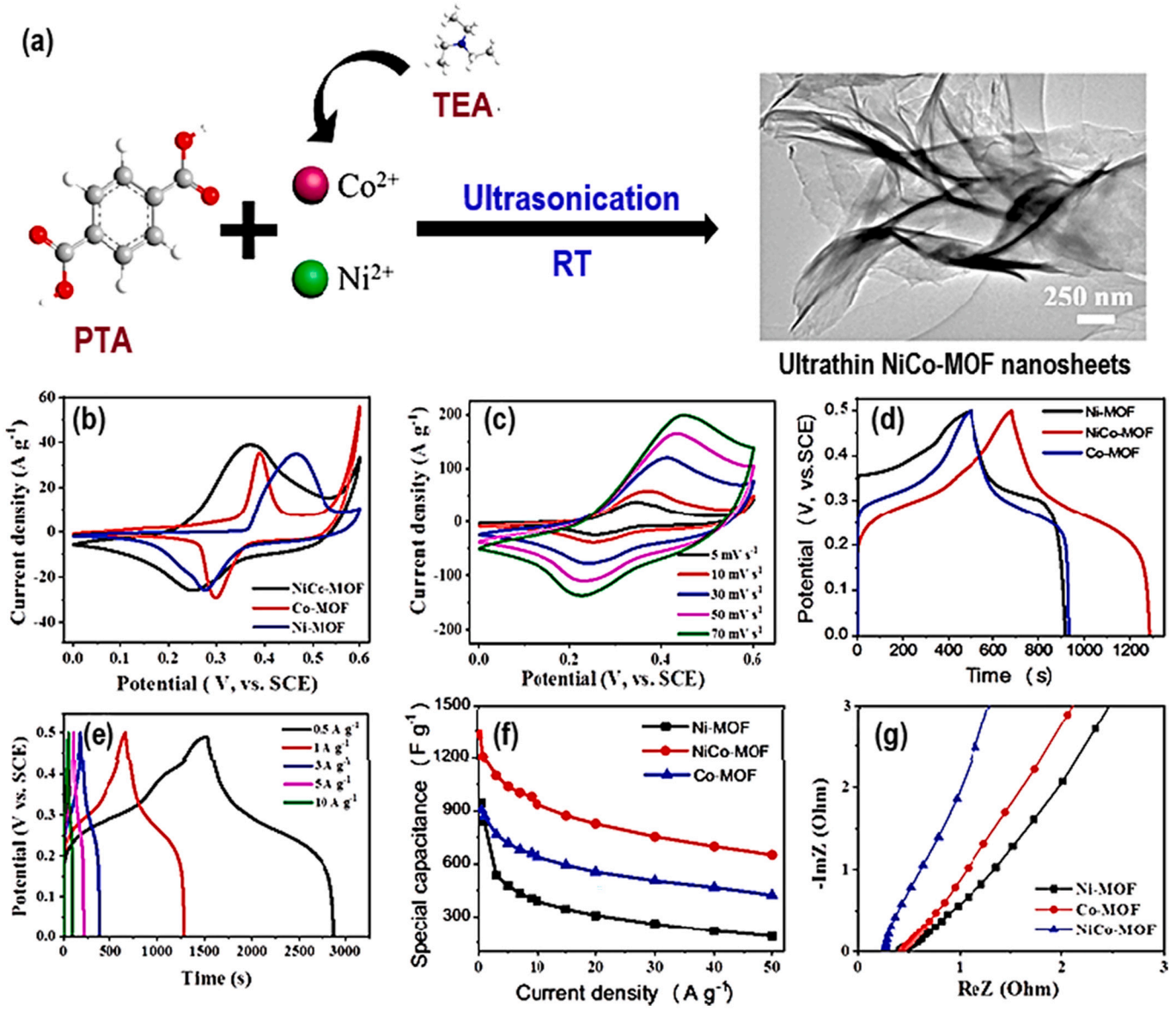

Fig. 6. (a) Scheme showing the synthesis of ultrathin NiCo-MOF nanosheets via the ultrasonication method at room temperature. (b) Curves for the CV at a 10 mV/s scan rate. (c) CV plot for the NiCo-MOF. (d) GCD profiles at a 1 A/g current density. (e) GCD profiles of NiCo-MOF. (f) Specific capacitances at varying current densities. (g) Nyquist plots of the MOF-based electroactive components. Adapted with permission [32]. Copyright (2019), American Chemical Society.

in Fig. 8e, indicate the pseudocapacitive characteristics of the MOFs. It was found that for the Ni-MOF fabricated at 180 °C while using HCl as the modulator, the pseudocapacitance was approximately 1457.7 F/g at 1 A/g whereas the pseudocapacitance for the Ni-MOF@GO was determined to be approximately 2192.4 F/g when applying a current density of 1 A/g with graphene oxide contents of 3 wt%. The addition of GO nanosheets also enhanced the cycling performance, with a retention of 85.1% being realized from an original value of 83.4% as shown in Fig. 8g. It should be noted that the pseudocapacitance of just the Ni-MOF on its own is quite large, resulting from the regular nanosized channels inherent to the structure of the designed framework facilitating high flux of electrolyte as well as electron transport during the process of charge/discharge. Additionally, the conditions to synthesize the Ni-MOFs were found to widely affect their electrochemical performance as they lead to significant changes to the structure and morphology of the MOF, which lead to the choice of the Ni-MOF fabricated at 180 °C with HCl as the modulator as this MOF exhibited the best crystallinity and highest specific capacitance. The increase of pseudocapacitance exhibited by the Ni-MOF@GO is substantial and can be attributed to the flower-resembling structure of this MOF composite facilitating effective use of the accessible active sites within the electrode as well as provision of channels for rapid transport of electrolyte. This structure is shown in Fig. 8b, c, and d.

Wang et al. fabricated a flower-resembling multi-walled carbon nanotube/nickel trimesic acid MOF composite (MWCNT@Ni(TA)) for use as a cathode material for energy storage [41]. The MOF and MOF composite (Ni(TA) and MWCNT@Ni(TA) respectively) were fabricated via solvothermal synthesis. MWCNT@Ni(TA) showed a specific capacitance of 115 mAh/g at 2 A/g. This was attributed to the tailored porous morphology of the Ni(TA) MOF, which increased the specific overall surface area of the composite while increasing the electrolyte/electrode interface contact. Also, the MOF's structure facilitates a high rate of electron/ion transfer by reducing the distance over which this transfer takes place. The multiwalled carbon nanotubes are shown, via morphological characterization, to connect the Ni(TA) nanosheets which increases the mechanical strength of the resulting MOF

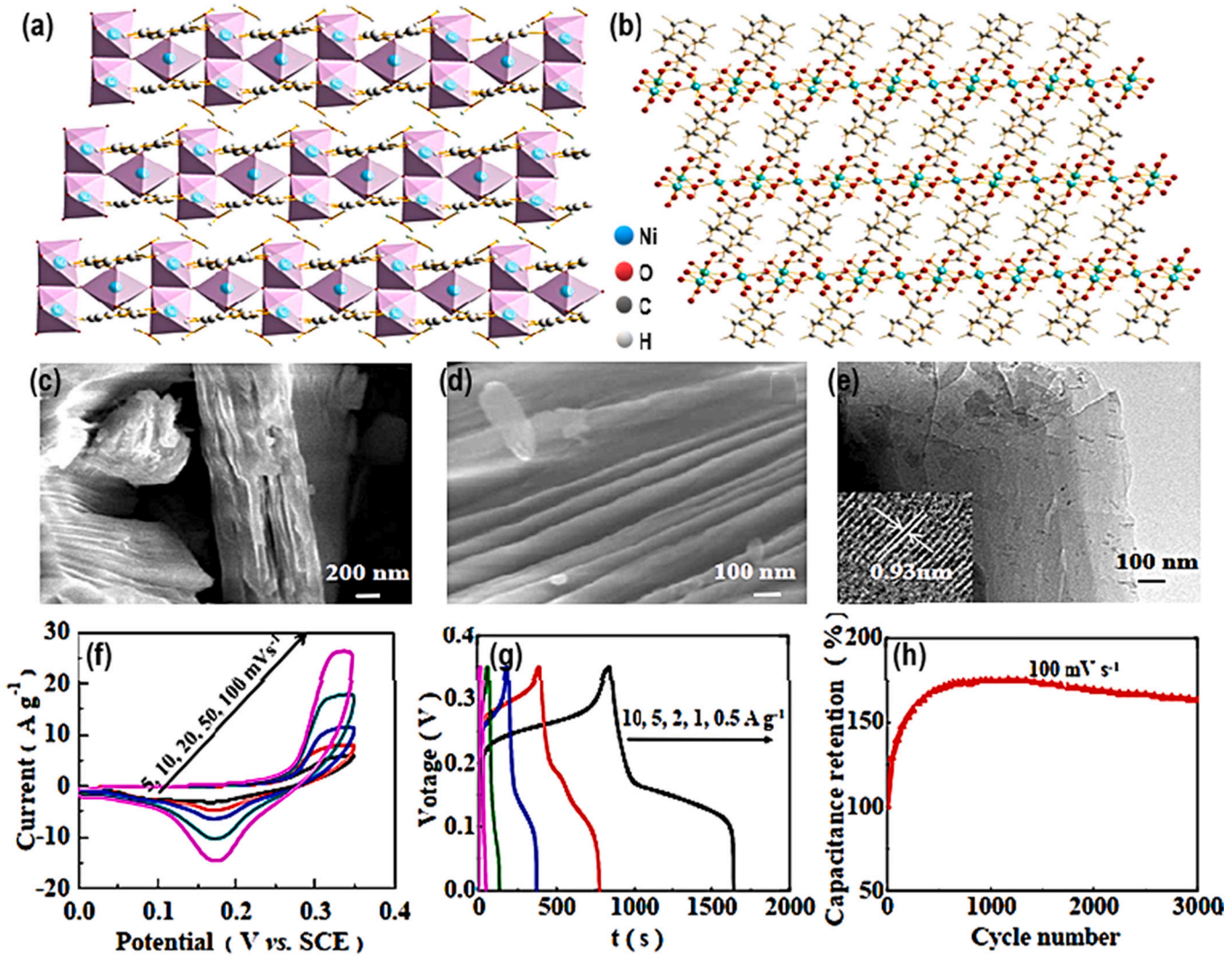

Fig. 7. (a) Chemical structure for the Ni-MOF-24 along the *a*-axis. (b) Structure of synthesized Ni-MOF-12 along the *b*-axis. (c-d) SEM micrographs for Ni-MOF-24. (e) images for TEM of the Ni-MOF-24 (HRTEM image inset). (f-h) Electrochemical analysis for the synthesized Ni-MOF-24 electrode: (f) CV curves, (g) GCD profiles, and (e) CV cycling performance. Adapted with permission [39]. Copyright (2014), The Royal Society of Chemistry.

composite. This increase is crucial in the prevention of the collapse of the composite while the charge/discharge process is occurring. The MOF itself also exhibits excellent bonding to the MWCNT leading to the observed superior properties of the overall composite.

Another study carried out by Choi et al. sought to demonstrate that nanocrystal MOFs (nMOFs) incorporated with graphene could be used in devices to serve as a supercapacitor [44]. To this end, 23 nMOFs were synthesized and tested. The synthesized nMOFs were of multiple metallic centers and organic linkers, differing shapes and pore sizes, different nanocrystal sizes, and varying types of structures. Fig. 9a shows a schematic of the construct for incorporating nMOFs into supercapacitors. It can be observed that the construct is based on placing the graphene-doped nMOF films (Fig. 9c) on either side of a separator membrane, followed by immersion into an electrolyte solution. Electrolyte ions are then free to move into and out of the MOF pores when an electric charge is applied. The performance of each nMOF varied with several of the fabricated MOFs exhibiting high capacitance values, the best of which was a zirconium MOF (nMOF-867) with an areal capacitance of 5.09 mF/cm^2 and stack capacitance of 0.64 mF/cm^2. This can be attributed to the high porosity of the structure of the MOF which facilitates the strong cycling of electrolyte ions within the supercapacitor as well as providing a large capacity for ion storage. Furthermore, the sp^2 N atoms in nMOF-867 enhanced the device performance by contributing to the increase in the interaction with the ions present significantly. Fig. 9b shows a simple schematic of the synthesis of nMOF-867 as well as an SEM image showcasing the porosity of the synthesized MOF. The Zr MOF exhibits higher energy density than activated carbon while also preserving its performance up to at least 10,000 cycles as shown in Fig. 9e and f.

3.2. *MOFs for batteries*

This section explores MOFs in lithium-ion, metal-sulfur, and metal-air for batteries. First, the working mechanisms of each of these types of batteries will be described in brief. Following this brief description, the application of MOFs in each of the battery types will be explored to show the role that MOFs play in improving the electrochemical properties of these devices.

Li-ion batteries are comprised of three main components, namely: (i) the anode, which is typically made from carbon; (ii) the cathode, typically a metal oxide; and (iii) the electrolyte, which is a lithium-based salt dissolved in an organic solvent [45]. Lithium-ion batteries are based on the insertion and disinsertion mechanism. During intercalation, Li ions move into the electrode and during deintercalation, the lithium ions

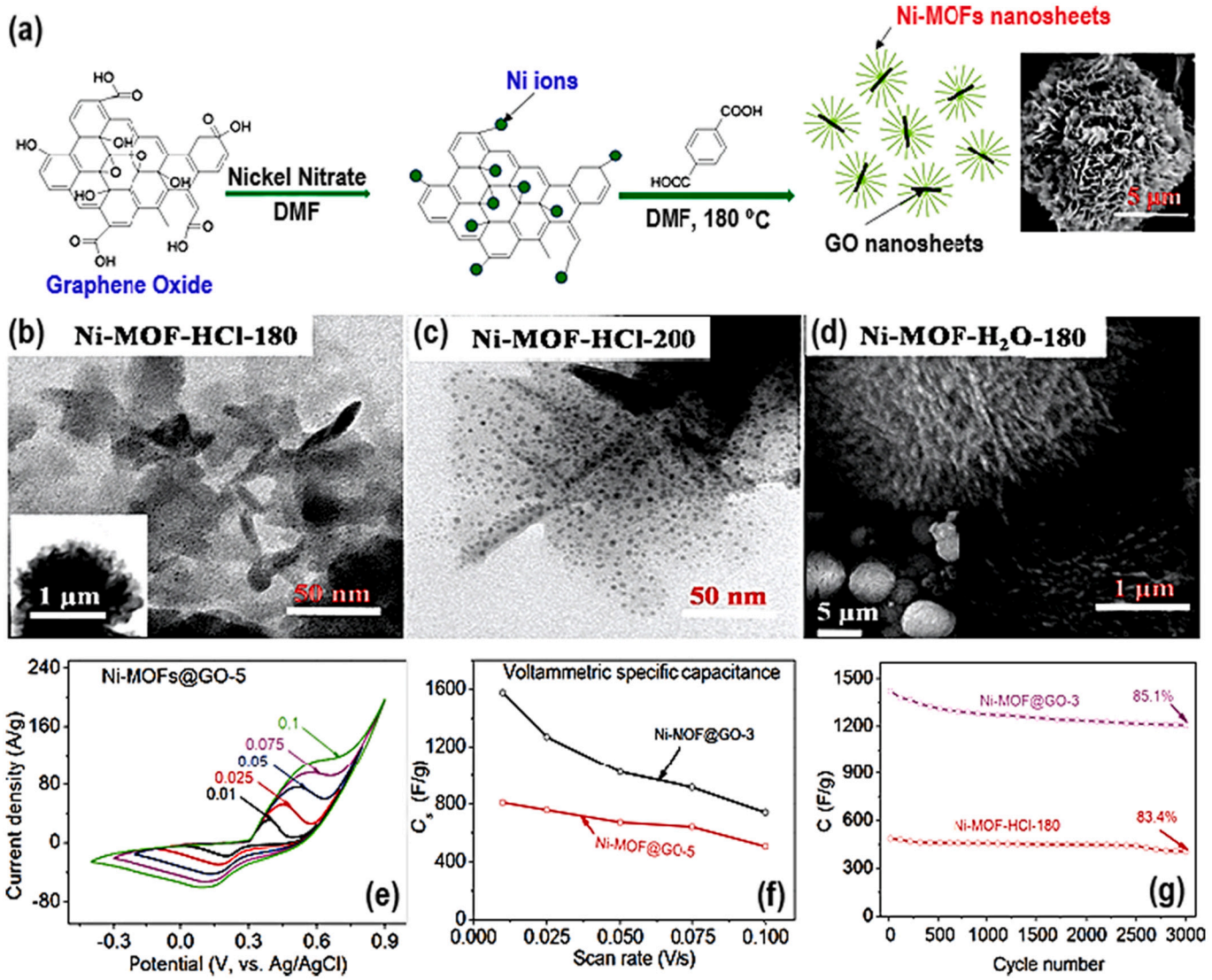

Fig. 8. (a) Schematic showing the in-situ synthesis of Ni-MOF hybrids with GO 2D nanosheets. TEM (b-e) and SEM (d) images of the synthesized samples with varying amounts of GO showing the unique flower-like structure. (e) CV profiles for Ni-MOFs@GO-5 sample at varying scan rates. (f) Voltametric specific capacitance curves of Ni-MOF@GO with varying GO contents. (g) Capacitance cycling performance of Ni-MOF@GO-3 and Ni-MOF-HCL-180. Adapted with permission [40]. Copyright (2016), American Chemical Society.

move out of the electrodes. As such, the materials chosen for the battery's anode and cathode are materials that facilitate the movement of lithium ions into and out of the electrodes. During discharging, the lithium ions are drawn out of the anode and move to the cathode where the insertion process occurs. The reverse happens during charging, whereby lithium ions are drawn out of the cathode and inserted into the anode. Fig. 10a shows a scheme for the working mechanism of a lithium-ion battery.

Metal-sulfur batteries have drawn great interest recently as energy storage devices. In particular, Li-S batteries (LSBs) have been the subject of extensive research due to their high theoretical energy density of about 2600 Wh/kg as well as their high theoretical capacity of about 1672 mAh/g [17]. The use of S also has several benefits such as low effects on the environment, high natural abundance, and low cost, making metal-sulfur batteries to be promising energy storage devices. LSBs will be the focus of this review, however, the working mechanism described applies to all metal-sulfur batteries. The LSBs have Li metal as the anode and elemental S as the cathode, with the electrolyte being an organic solvent [46]. During discharge, the lithium anode dissolves into the electrolyte releasing lithium ions. These ions move to the cathode where the reaction with S occurs to form polysulfide molecules. When charging, the polysulfide ions decompose and the released lithium ions move back to the anode [47].

Metal-air batteries (MABs) are based on a metal anode, a porous air cathode that allows surrounding air to be absorbed into the device, and a separator [47,48]. Fig. 11a shows theoretical values of several electrochemical performance parameters for varying MABs, with lithium showing the best theoretical combination of the highest theoretical energy density with a high nominal cell potential. MABs can be classified according to the nature of the electrolyte used, with the two major electrolyte systems used being aqueous electrolytes and non-aqueous electrolytes. For aqueous electrolyte systems, the metallic anode is oxidized to release electrons and metal ions. During discharging, these metal ions react with hydroxide ions forming metal hydroxides [48]. The released electrons engage in the oxygen reduction reaction (ORR) where the absorbed oxygen molecules are reduced to hydroxide ions through their combination with the electrons and water. The process is similar for non-aqueous electrolyte systems with the difference being that instead of the oxygen being reduced to hydroxide ions at the cathode, oxygen instead receives the electrons and combines with them

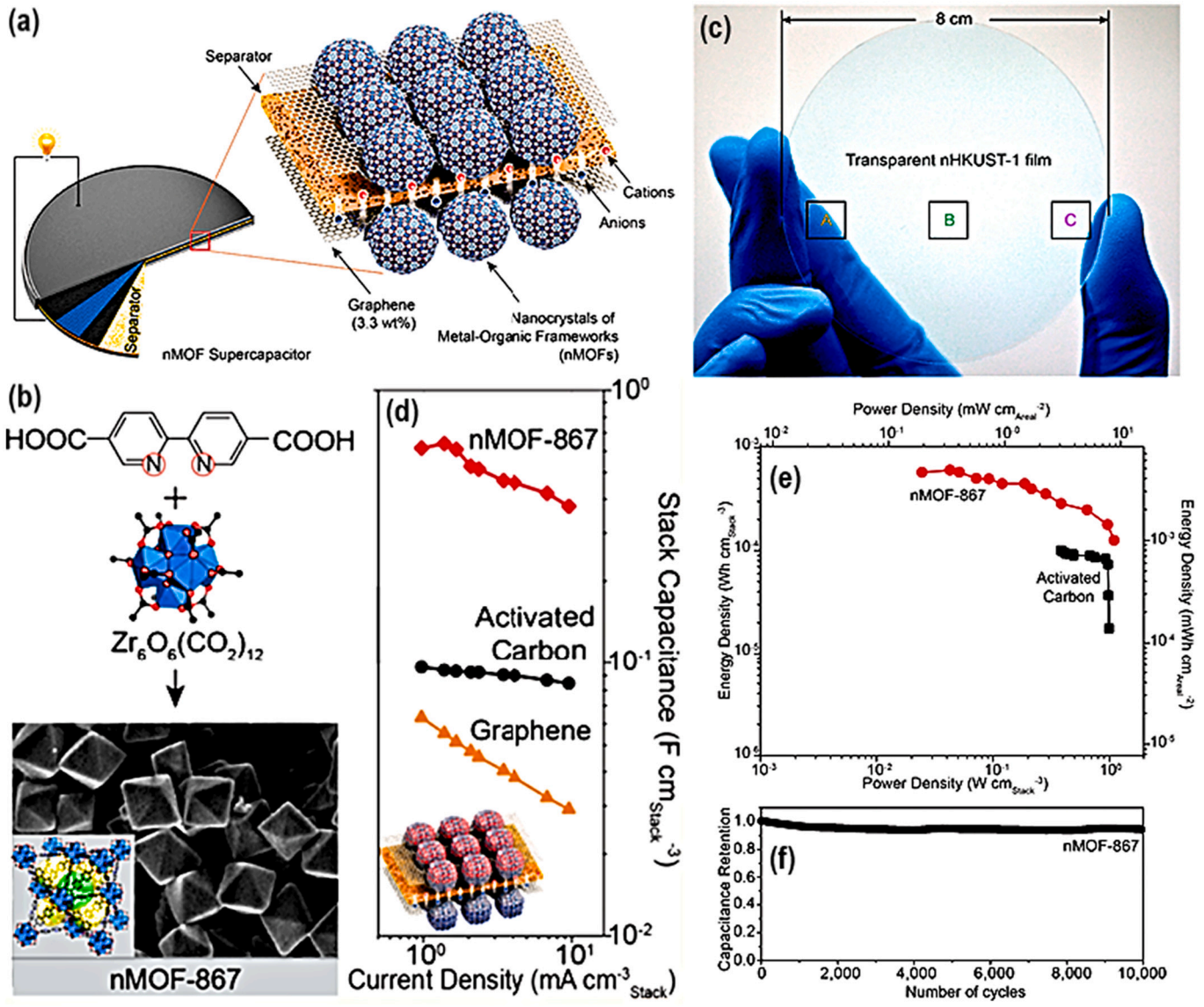

Fig. 9. (a) scheme showing the construct of incorporating nMOFs into supercapacitors. (b) Synthesis schematic and SEM image of nMOF-867 (c) A nHKUST-1 transparent film over a quartz as substrate with a radius of 4 cm. (d) Volumetric stack capacitance of nMOF-867 compared to that of graphene and activated carbon (e) Ragone plot of nMOF-867 compared to those of activated carbon and cycle life of synthesized nMOF-867. (f) Stability performance of the MOF. Adapted with permission [44]. Copyright (2014), American Chemical Society.

to form oxygen anions [47]. Fig. 11b shows a schematic of these two electrolyte systems applied in MABs.

Moving on to the application of MOFs for batteries, several studies have been carried out to this end in recent years. Table 3 presents an overview of the major findings of the studies reviewed herein. Maiti et al. carried out a study in which an Mn-BTC MOF was applied as an anode material for a Li-ion battery [49]. The MOF was obtained via a simple solvothermal process and this is the first time this particular MOF has been applied as an anodic material. The study reports that for a potential range of 0.01–2 V versus Li/Li^+, the MOF anode showed high specific capacity values of around 694 and 400 mAh/g at a current density of 0.1 and 1.0 A/g, respectively. In addition to this, the MOF exhibits good retention of its capacity, good cyclability, and good stability. The MOF shows promise as an anodic material beyond the 2 V potential.

In another study conducted by Jin et al., a composite based on Fe-MOF/reduced graphene oxide (RGO) was synthesized and again applied as an anode for a Li-ion battery [50]. This MOF composite was synthesized via the solvothermal approach, as seen in the schematic in Fig. 12a. The study shows that the Fe-MOF/RGO composite with 5 wt% RGO (Fe-MOF/RGO (5%)) displayed excellent storage of lithium ions as well as a reversible capacity of 1010.3 mAh/g that could be cycled around 200 cycles along with a superior rate performance. Fe-MOF/RGO (5%) also displayed a high initial charging and discharging capacity of 891.1 and 2055.9, respectively, and an initial coulombic efficiency of 43.3% as seen in Fig. 12e and f. It was suggested that the RGO coating on the Fe-MOF prevented the electrode and the electrolyte from coming into direct contact. Fig. 12b and c show SEM images of the morphology of the as-prepared MOFs, with Fig. 12c showing the coating of the Fe-MOF particles by the RGO nanosheets. Fe-MOF contributes excellent redox activity and stability to the overall composite, while also possessing a high theoretical capacity. The synergistic effect of the MOF, which has a high theoretical capacity, and RGO, with high conductivity, are what contribute to this excellent electrochemical performance. For both of these examples, the MOF's tunable structure and pore sizes work in combination to facilitate improved ion diffusion leading to the observed improvement in the overall electrochemical performance [17].

Li et al. [51] took advantage of the tailorable morphology of MOFs

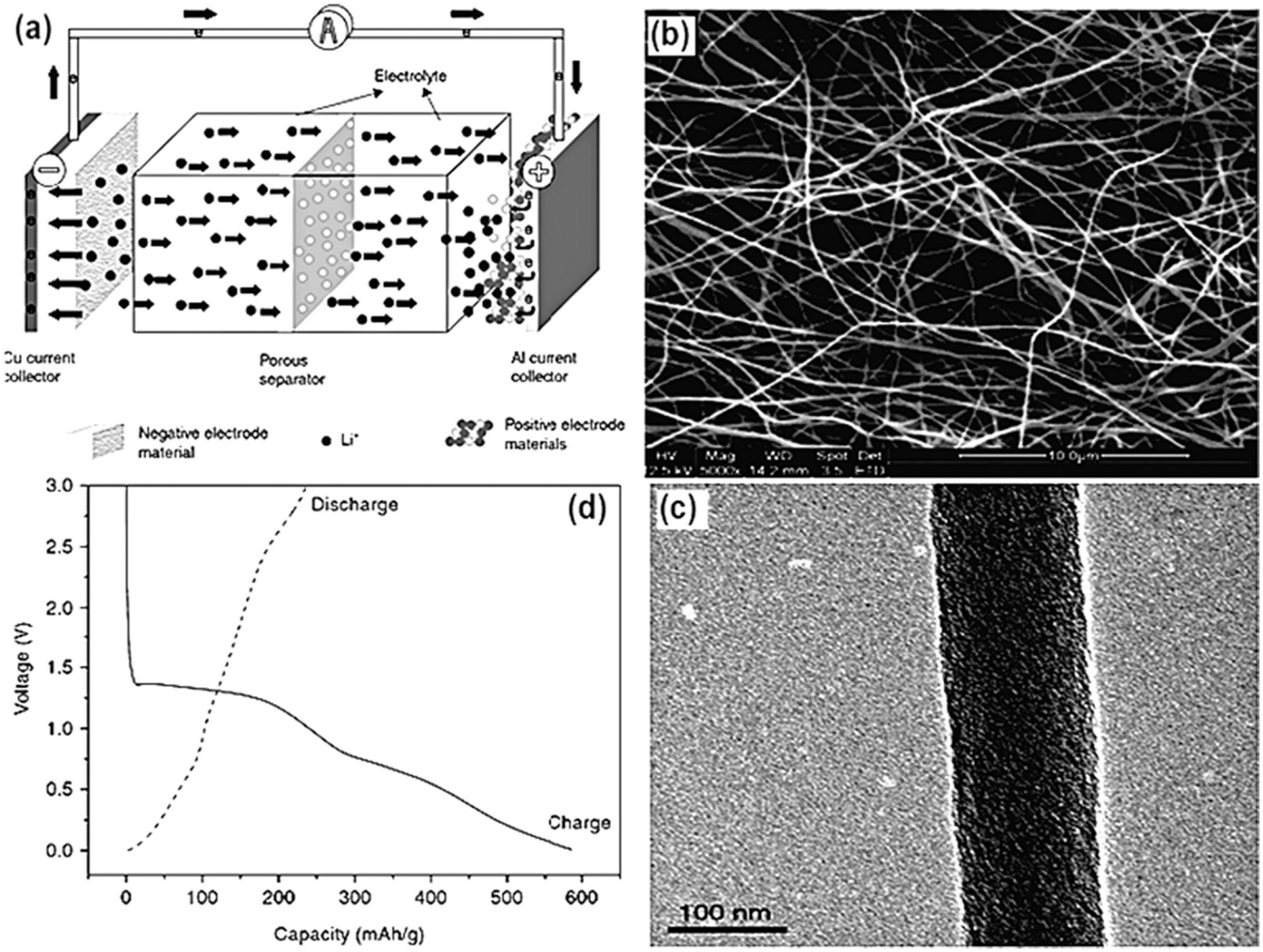

Fig. 10. (a) Scheme showing the working mechanism of a lithium-ion battery. Scanning electron microscopy (SEM) (b) and transmission electron microscopy (TEM) (c) images of porous carbon nanofibers. (d) Initial discharge-charge curves for porous carbon nanofiber electrodes used in a lithium-ion battery. Adapted with permission [45]. Copyright (2012), Elsevier.

synthesizing Cu-based MOFs with a *Hericium erinaceus*-like shape to be utilized as anode materials in high-performance Li-ion batteries. By introducing polyvinylpyrrolidone (PVP) as a structure tuner, the stacking arrangement of the MOF nanosheet was modified to a *Hericium erinaceus* hierarchical structure type of morphology. This MOF morphology facilitated the provision of abundant and short paths transportation for Li-ion diffusion thereby improving the electrode's conductivity. In addition to this, the electrode's structural stability was enhanced while also reducing the stress on the electrode during the discharging and charging process thus contributing to long-cycle performance. Furthermore, the moderate MOF's surface area led to an effective alleviation of side reactions that typically plague LIBs, leading to a stable SEI overall. As a result of these factors, the discharge capacity was 1205.9 mAh/g initially at 100 mA/g of current density. After 150 cycles, the discharging capacity was retained at 897 mAh/g, thus exhibiting satisfactory electrochemical performance.

Also, MOFs along with MOF-derived materials have been utilized in Na-ion batteries. In a study by Pan et al., a porous CuO/RGO-based composite was synthesized via pyrolysis of Cu-based MOFs/GO to be utilized as an anode component for Na-ion batteries [59]. These composite materials showed 466.6 mAh/g of specific capacity at 100 mA/g of current density after 50 cycles. The MOF presented a conductive network structure as a result of being a MOF-derived composite, as well as the inhibition of the CuO nanoparticle's aggregation with RGO, which was the driving factor for the diminishment of the resistance to charge transfer and the subsequent enhancement in overall electrochemical properties. Ramaraju et al. synthesized a Cu-MOF-derived hollow polyhedron functionalized with GO [60]. The composite was utilized as an anode material for Na-ion batteries. The synthesis process was facile sintering of Cu-MOF which was embedded with exfoliated graphene. The composite exhibited excellent electrochemical performance, with a reversible capacity maximum of 1490 mAh/g after 220 cycles being realized. The utilization of the Cu-MOF-based composite electrode leads to an overall reduction in cell resistance, as the copper offers high Li^+ diffusion coefficients along with a large contact surface area between the electrode/electrolyte interface. This thus leads to the quick absorption and storage of vast amounts of Li ions without decaying in the electrode's performance.

The use of MOFs in potassium-ion batteries has also attracted research attention in recent years. Tang et al. carried out density functional theory (DFT) as first-principles computations to determine the performance of UiO-66 MOF as an anode component for K-ion batteries [61]. UiO-66 MOF was determined to have 644 mAh/g of maximum specific capacity when utilized as the anode of a K-ion battery. The maximum migration energy barrier for potassium during diffusion along the UiO-66 framework was determined to be 0.377 eV, which is much lower than those of sodium and lithium diffusion in the same MOF anode. UiO-66 does not experience any changes in frame structure

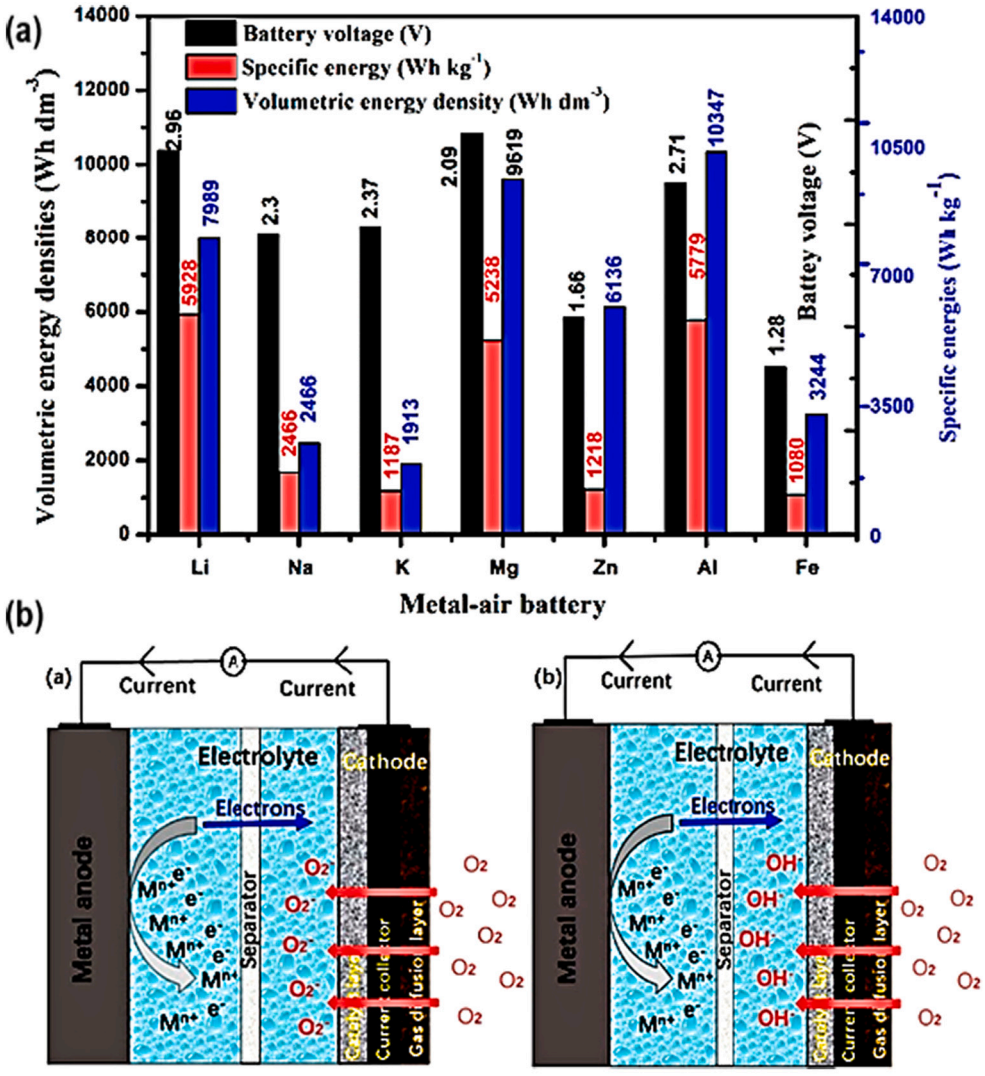

Fig. 11. (a) Theoretical specific energies, nominal battery voltages, and volumetric energies of different metal-air batteries (b) Schematic showing the working mechanisms of MABs for non-aqueous electrolyte (left) and aqueous electrolyte (right). Adapted from reference [47]. The article is distributed under a Creative Commons Attribution License 4.0 (CC BY).

Table 3
Overview of MOF and MOF-based materials and their properties suitable for battery use compared to other electrocatalysts.

Material	Synthesis method	Battery type	Discharge capacity	Reference
Mn-BTC MOF	solvothermal	Li-ion	400 mAh/g	[49]
Fe-MOF/RGO	solvothermal	Li-ion	1010.3 mAh/g	[50]
HECM	hydrothermal	Li-ion	1205.9 mAh/g	[51]
S-MOF-5	modified room temperature precipitation	Li-sulfur	1476 mAh/g	[52]
MOF-74-Ni/CNT	hydrothermal	Li-sulfur	773 mAh/g	[53]
Ni-Co-S/NSC	room temperature precipitation	Metal-air	829 mAh/g	[54]
FeS/Fe_3C@NS-C-900	solvothermal	Metal-air	750 mAh/g	[55]
LiIL-MOF	mechanochemical	Metal-air	500 mAh/g	[56]
$CuFeS_2$ nanosheets	solvothermal	Na-ion	528 mAh/g	[57]
V_2O_3/C nanocomposite	solvothermal, calcination	Na-ion	216 mAh/g	[58]

during potassium insertion, Additionally, the diffusion coefficient of potassium in UiO-66 is larger than those of sodium and lithium by several orders of magnitude, thus confirming that potassium ions are favored when UiO-66 was utilized as an anode component, making the MOF material a promising candidate for utilization in potassium-ion batteries. Zuo et al. synthesized a MIL-88A-derived with porous carbon and S-doped for application as a K-ion battery anode [62]. The resulting material has a flower-like structure which is obtained from the unique morphology of MIL-88A. The synthesized material exhibited a 3D open framework, thus facilitating the provision of a large specific area which shortens the K^+ transport path as well as an increase in (i) the active sites' number and (ii) the interlayer spacing. As a result, the synthesized material displayed excellent electrochemical performance, with a high reversible capacity of over 358 mAh/g and a rate performance of 192.6 mAh/g at a current density of 2 A/g.

LSBs, as previously mentioned, have high theoretical energy and a

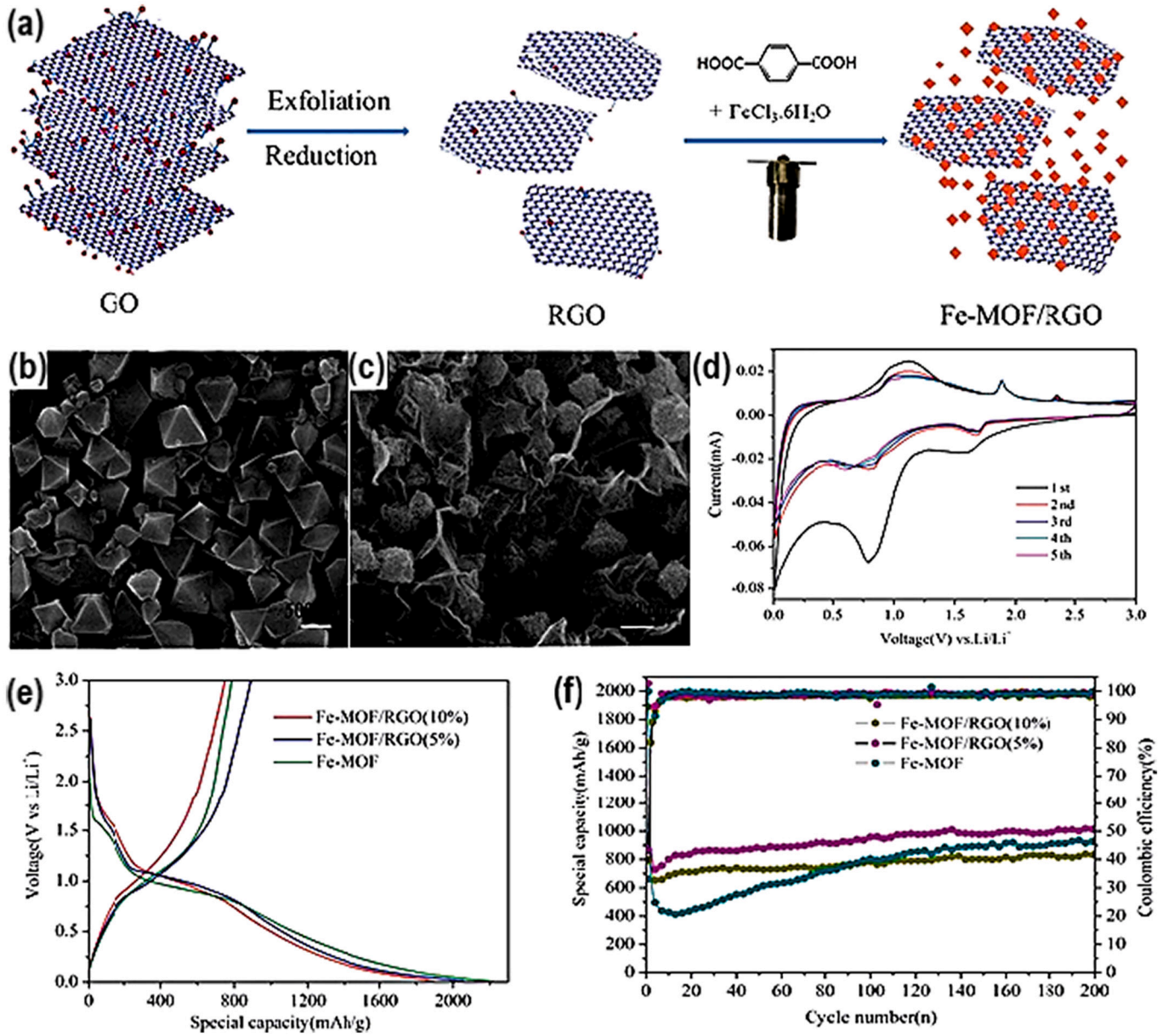

Fig. 12. (a) Synthesis schematic showing the Fe-MOF/RGO composite via solvothermal synthesis method. (b) SEM micrographs of Fe-MOF and (c) Fe-MOF/RGO composites. (d) CV plots for the first 5 cycles for Fe-MOF/RGO (10%). (e) Charge and discharge curves of Fe-MOF, Fe-MOF/RGO (5%), and Fe-MOF/RGO (10%). (f) Coulombic efficiency and cycling performance of Fe-MOF, Fe-MOF/RGO (5%), and Fe-MOF/RGO (10%). Adapted with permission [50]. Copyright (2010), The Royal Society of Chemistry.

large theoretical capacity. However, LSBs have not been practically applied despite their promising potential as an energy storage component. This is due to (i) the insulating properties of both the sulfur and the sulfur discharge products causing slow electrochemical kinetics; (ii) internal shuttling caused by the solubility of polysulfides' long chain in the electrolyte, inhibiting the charging efficiency while causing the capacity to fade; and (iii) cathode pulverization causing large volume variations during the charging/discharging processes leading to fading of capacity [17]. Extensive research has thus been conducted on the application of MOFs for these batteries, with promising results. Shanthi et al. conducted a study in which a MOF-5-contained sulfur material (S-MOF-5) was synthesized and used as a cathode material for an LSB [52]. Fig. 13a shows a scheme of the synthesis method for the MOF-5 and the incorporation of sulfur into the MOF's structure. The highly porous structure of the MOF-5 is shown in Fig. 13b. The synthesized cathodes exhibited an initial specific capacity of 1476 mAh/g, which then stabilized to about 609 mAh/g after 200 cycles. The capacity fade rate was negligible at 0.0014% cycle^{-1}. This is in stark contrast to commercial sulfur which, as shown in Fig. 13d, faded to less than 100 mAh/g from the initial capacity of around 800 mAh/g in less than 20 cycles. Incorporating MOF-5 prevented polysulfide dissolution to some degree, which made these cathode materials the most promising candidate for application in LSBs.

In another study, Xu et al. synthesized MOF-74-Nickel/carbon nanotube (MOF-74-Ni/CNT) composite to be an S host for LSBs [53]. The composites were synthesized via a hydrothermal process shown in Fig. 14a after which sulfur was incorporated into the composite via impregnation. Fig. 14b and c showed the morphology of the MOF-74-Ni/CNT before and after sulfur impregnation. The study reported that the battery exhibited 773 mAh/g as its initial discharge capacity, which stabilized at 503 mAh/g after 400 cycles at 2C. The capacity fade rate was low at a value of 0.087% per cycle. Also, at 0.5C, the battery

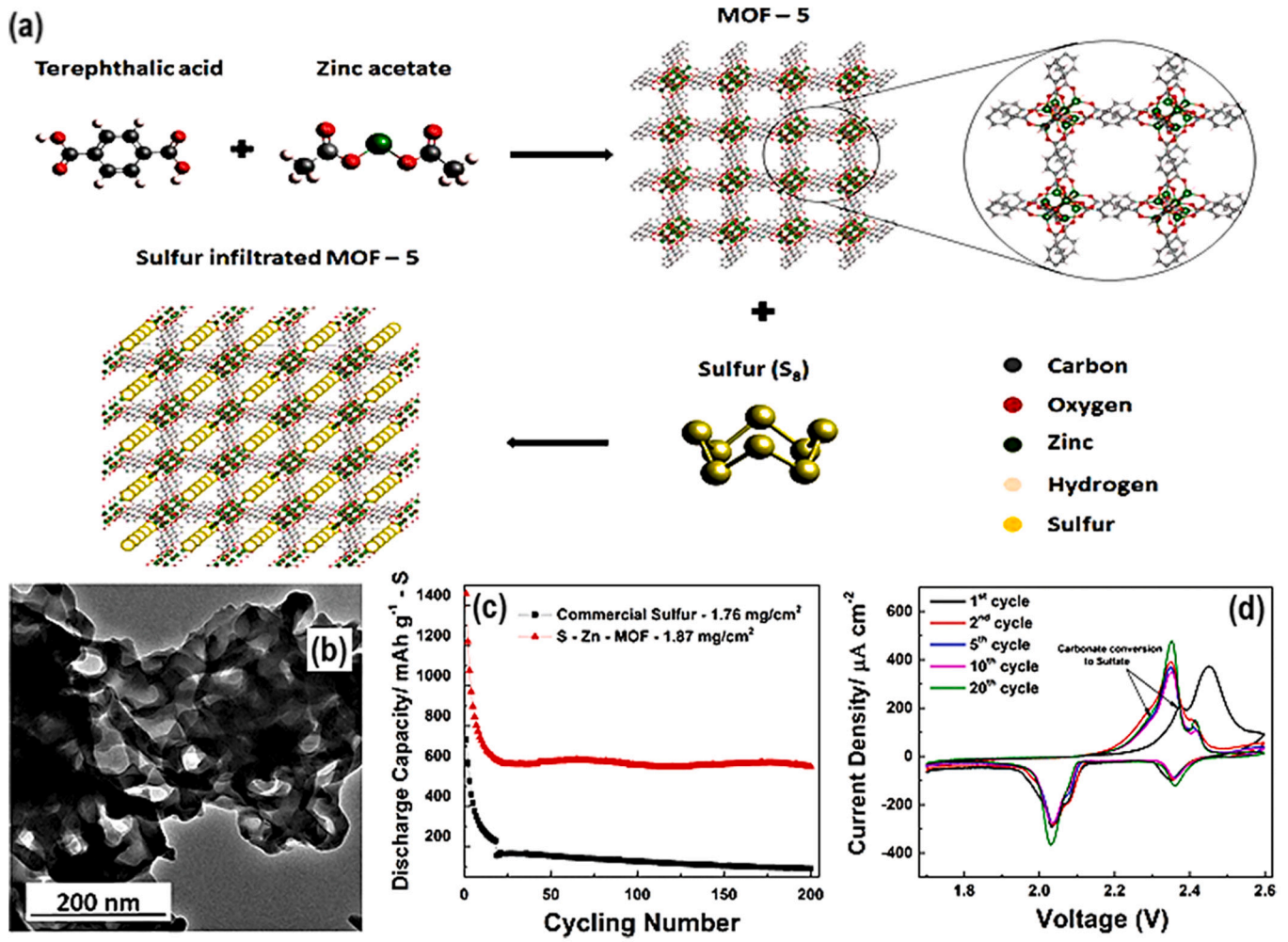

Fig. 13. (a) Scheme showing the synthesis of MOF-5 and the following incorporation of sulfur into the MOF structure via infiltration. (b) TEM image of Zn-MOF-5 W. (c) Cycling performance of commercial sulfur and S-Zn-MOF. (d) CV curves of S-Zn-MOF at 1st, 2nd, 5th, 10th and 20th cycles. Adapted with permission [52]. Copyright (2017), Elsevier.

exhibited an initial discharge capacity of 1065 mAh/g and maintained a discharge capacity of 640 mAh/g after 100 cycles, as is shown in Fig. 14e. The selection of MOF-74 proved to be a major contributor to the excellent electrochemical performance, as it provides plenty of active metal sites which facilitate significant interactions with the polysulfides. Ni-MOF-74 was also more stable when compared to other MOF-74-based materials. Additionally, the MOF-74 structure also exhibits long-range electric contact. These factors, in combination with the high affinity for polysulfide ions by MOF-74-Ni, lead to the observed electrochemical performance of the resulting LSB.

For metal-air batteries, the oxygen evolution reaction (OER) and ORR are crucial for their operation. These reactions are plagued with slow kinetics and as such employ the use of catalysts such as platinum, RuO_2, and IrO_2. However, these catalysts are rare and costly, which limits their industrial application. MOFs are strong candidates for OER/ORR catalysts due to their tunable structure and diverse compositions. As such excessive research has been conducted in recent years on the applications of MOFs as electrocatalysts and subsequently their applications in metal-air batteries. Wu et al. conducted a study in which Ni-Co-MOF was sulfurized at low temperatures to yield a Ni-Co-based sulfide coupled with N and S-codoped on carbon support composite (Ni-Co-S/NSC) that can be employed as a cathode component in a rechargeable Zn-air battery [54]. A Zn-air battery with this material at the cathode exhibited satisfactory electrochemical properties with 829 mAh/g of specific capacity and a peak power density of 137 mW/cm^2. This performance was attributed to the proper OER, and ORR performance exhibited by the MOF composite (10 mA/cm^2 at 309 mV and 0.81 V at $E_{1/2}$ respectively), a result of the porous and multichannel nanostructure of the MOF composite. In situ Raman spectra revealed that the formation of metal hydroxides during OER facilitated the endowment of the synthesized electrocatalyst with excellent electrocatalytic properties. In another report, Li et al. fabricated a honeycomb-like Fe-MOF-derived composite (FeS/Fe_3C@NS-C-900) to be applied as air cathode material in a rechargeable Zn-air battery [55]. The honeycomb-like structure could be observed in the SEM images in Fig. 15b and c, with the synthesis of this Fe-MOF-derived composite shown in Fig. 15a. The Zn-air battery with the composite cathode exhibited 750 mAh/g of specific capacity and a power density maximum of 90.9 mW/cm^2 shown in Fig. 15d. The battery showed excellent stability over 1730 cycles at 2 mA/cm^2. The nanocomposite displayed a low potential gap (ΔE) of about 0.72 V, thereby confirming an efficient bifunctional electrocatalytic activity toward OER and ORR. This is brought about by the porous nature of the honeycomb-like MOF structure utilized in this composite, which provided ample exposed active sites for electrocatalytic activity. Specifically, the entry of O_2 and electrolytes was facilitated by this porous framework structure which offered robust support with targeted pores. Additionally, heteroatom doping is facilitated by the organic ligands present as they posess multiple atoms.

Liu et al. synthesized a MOF-based electrolyte to improve the cycling performance of Li-air batteries at elevated temperatures [56]. The

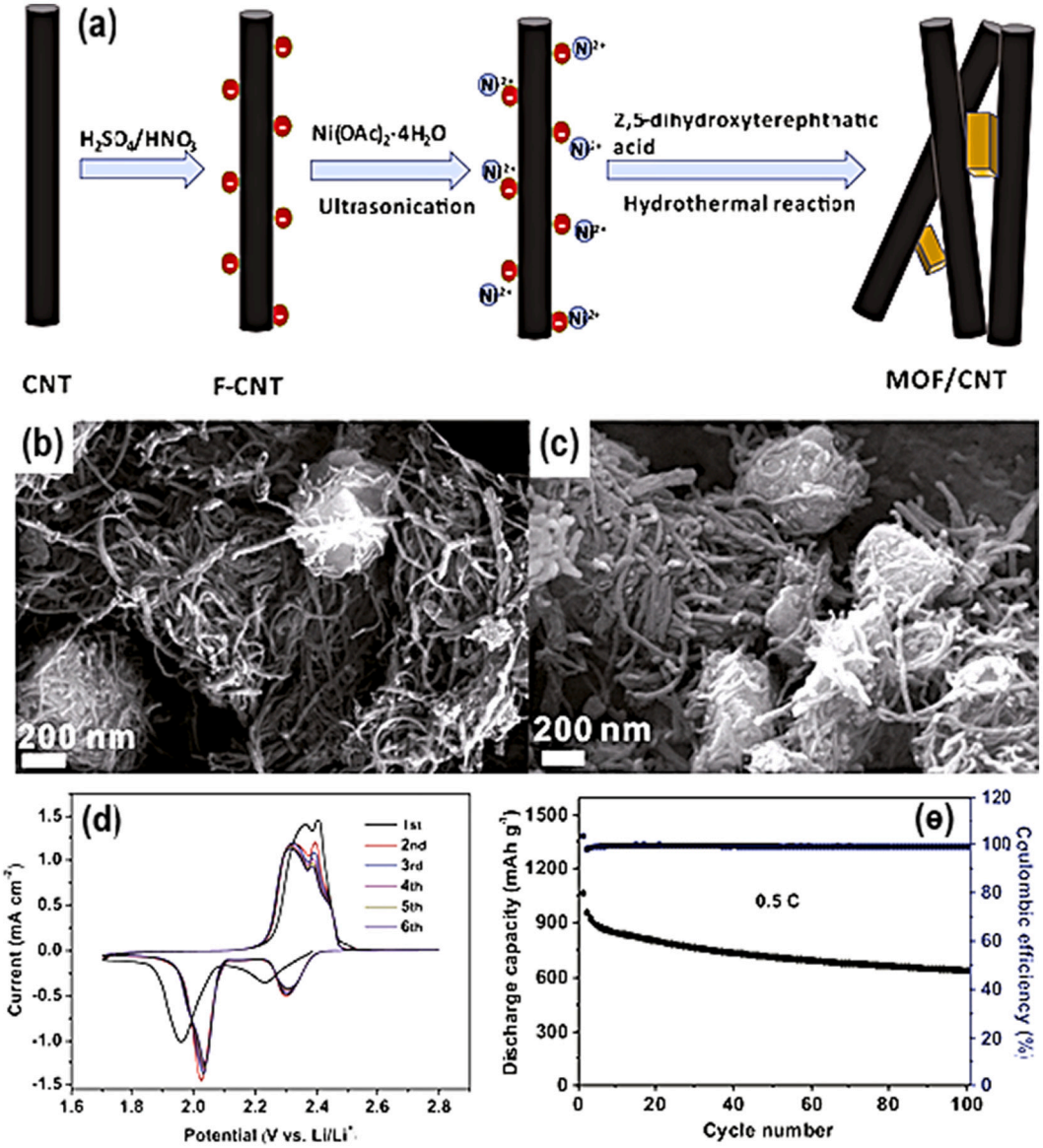

Fig. 14. (a) Scheme demonstrating the synthesis of MOF-74-Ni/CNT via the hydrothermal synthesis method. (b) SEM micrographs of the as-prepared MOF-74-Ni/CNT and (c) MOF-74-Ni/CNT/S. (d) Charge-discharge voltage profiles for the first 6 cycles. (e) cycle performance at 0.5C. Adapted with permission [53]. Copyright (2018), Elsevier.

electrolyte itself was based on a MOF and an ionic liquid and was utilized to improve interface stability by stabilizing the cathode and protecting the lithium cathode at high temperatures, thereby improving cycling performance at said elevated temperatures. This quasi-solid-state electrolyte forms a MOF-particle-rich layer that covers the lithium anode, which led to excellent contact and enhanced long-term cycling stability. Uniform deposition of Li and the prevention of Li dendrite propagation is facilitated by the MOF particles within the solid electrolyte by the regulation of homogenous Li^+ flux distribution. This, therefore, promoted the development of a stable solid electrolyte interphase layer as well as the prevention of cell failure by the propagation of lithium dendrites [56]. As a result of these factors, the assembled lithium-air battery exhibited a long cycling life of around 1100 h with a polarization of 0.5 V at 60 °C, with improved electrochemical performance being realized at 80 °C.

On the other hand, DFT investigations are critical for understanding the specifics of mechanisms, reaction pathways, geometrical and electronic structure, and how these factors affect electrochemical applications. DFT calculations were used on MIL-101 by Fatemeh Keshavarz et al., who also examined the Fe^{3+}/Fe^{2+} redox behavior in MIL-101(Fe) on secondary building units (SBU). The SBUs were revealed to represent the MIL-101's active sites [63] and are a viable replacement for the cluster model's extended periodic structure because they can enhance the binding characteristics close to the active sites (Fig. 16(a-b)). The Fe^{3+}/Fe^{2+} redox couple present in this MOF was found to be electrochemically active and thus leads to the MIL-101(Fe) undergoing reversible redox reactions on its structure. The findings revealed how redox reactions in this MOF work and made it possible to recognize irreversible Li-intercalation processes.

Recently, the electronic structure of MOFs was investigated, and proposed that the coulomb interaction impacts be significant at the transition metal atoms [65]. The electronic simulations were carried out using a cluster structure of the massive MIL-101(Fe) cell unit taken, a trimetallic MOF ($[Fe_3O(OOCH)_6L_3]^+$, where L is the ligand) with paddlewheel compound (Fig. 16c) [64]. Additionally, Trepte et al. [66] carried out the DFT calculation on DUT-8(Ni) using two primary methods: RESPECT (relativistic spectroscopy code), single-point energy assessments, and conventional quantum chemical modeling for

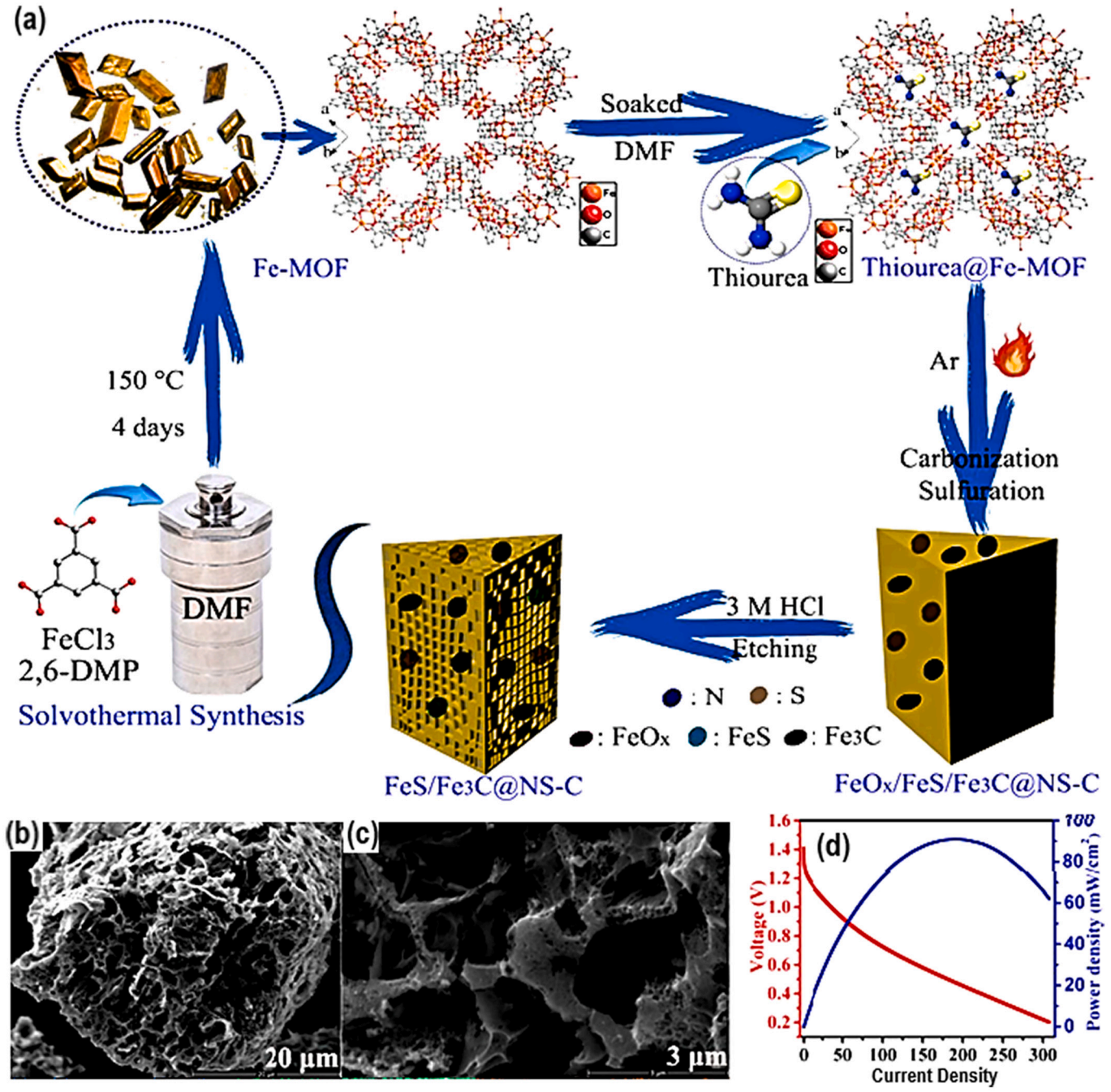

Fig. 15. (a) Scheme showing the synthesis process of honeycomb-like Fe-MOF derived composite material. (b-c) SEM images of honeycomb-like FeS/Fe_3C@NS-C-900 composite at different magnifications. (d) Discharge polarization and related power density curves of the Zn-air battery with FeS/Fe_3C@NS-C-900 composite as the air cathode. Adapted with permission [55]. Copyright (2020), American Chemical Society.

geometrical optimization and calculation of frequency with a Gaussian 16 revision A.03. It was demonstrated that the first electron's addition, or the intercalation of the first Li-ion, led to 2.79 V at the B3LYP/def2-TZVP level, as opposed 5.24 V in the ideal situation (with no geometrical distortion). When compared to the Li/Li^+ reference, the diminished peaks in the CV presented by Shin et al. [63] for a MIL-101(Fe) MOF that had Cl in the axial plane (MOF/carbon black weight ratio of 3:7) were at 2.99, 2.59, 2.42, 2.27, and 2.13 V. On the other hand, the corresponding peaks presented by Yamada et al. [67] for a water-bound MIL-101(Fe) that was blended with PTFE and Ketjen black adhesive were found at 2.94, 3.08, and 3.50 V. The value produced from this study was more practical (2.79 V) as compared to the ideal value of 5.24 V but is reasonably in accord with the experimental findings (Fig. 16d) [65]. The fact that the models of 2.79 V were lower than the theoretical voltage of 5.24 V showed that some of the energy acquired during the reduction process was lost during the deformation of the MIL-101(Fe) SBU when in presence of Li atoms. Such investigations indicate that DFT calculations can be useful for revealing the real reaction mechanism of charge storage with MOF-based materials.

3.3. *MOFs for flexible electrochemical energy storage devices*

Advances in the electrical energy field have continued to be a remarkable resource to humanity's power demands, which only continue to grow as the years go by. Developments in modern electronic devices have been significant, with the sector of flexible and portable

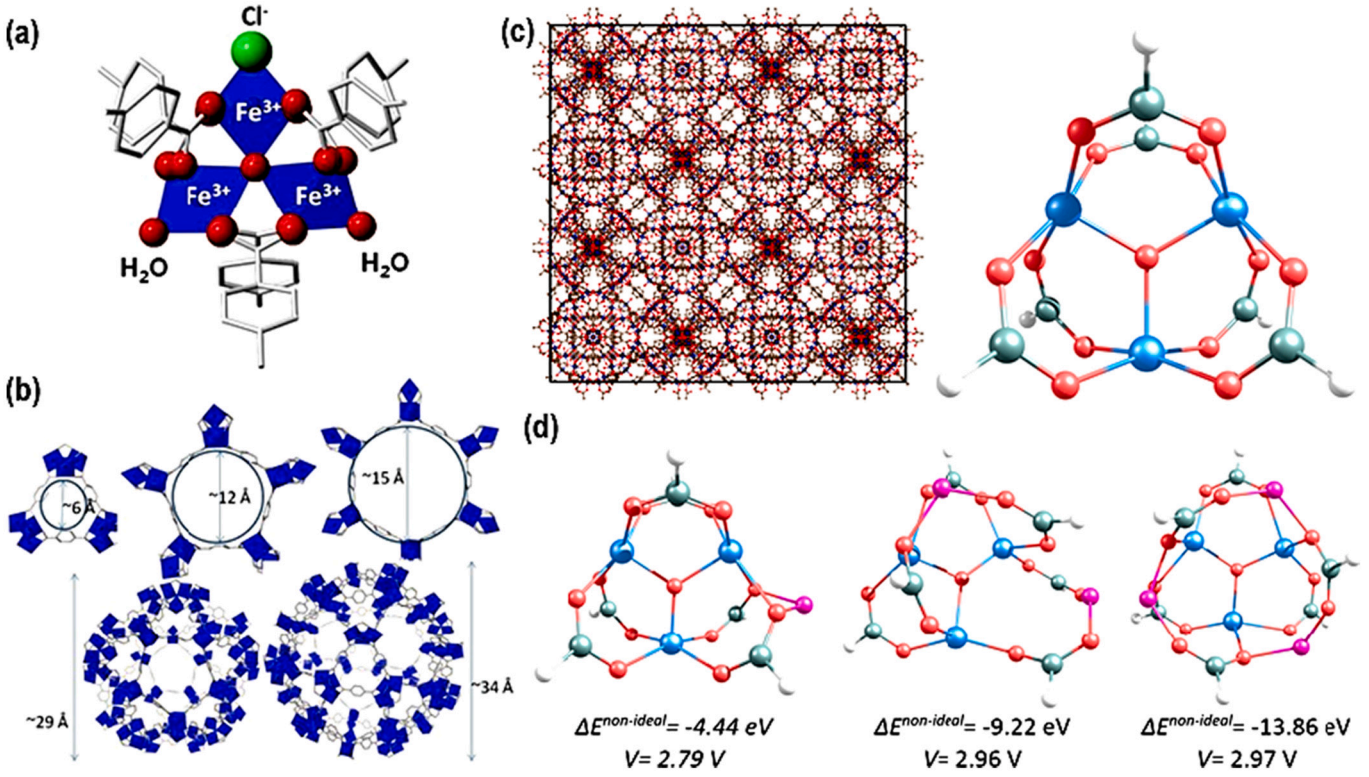

Fig. 16. Chemical representation of MIL-101(Fe) (a) SBU. (b) Pores and windows of MIL-101(Fe) [63]. (c) Cell unit for the MIL-101 crystal and the selected model structure. (d) Intercalation of 1 to 3 Li atoms (from left to right) into the structure of the MIL-101(Fe) model at B3LYP/def2-TZVP level. The electrochemical potential reported was calculated based on the reference to the Li anode [64].

electronic devices being an area of major attention. The demand for electronic devices with flexible, foldable, and stretchable functionalities is high for applications in wearable devices, e-skins, smartphones, and subcutaneous medical devices, to name a few [68]. Along the electrochemical energy storage devices, metal-ion batteries and supercapacitors have shown the most promise based on their superior energy storage features such as high cycle stability and power density [69]. However, traditional metal-ion supercapacitors and batteries tend to be rigid which thus limits their application in flexible and wearable electronics. As such, there is a requirement to obtain electrochemical energy storage components that are equally as flexible and stretchable to power these flexible electronic devices. Not only do these energy storage devices need to be flexible, but they also must be able to retain their electrochemical functions after being subjected to deformation and be lightweight [69]. MOFs can be applied in the manufacturing of materials suitable as electrodes for these devices, as their appreciable specific surface area, as well as large pore volume, facilitate both high charge storage capability (thus contributing to a higher overall capacitance) and high-power output, which is crucial for flexible electronics and electronics in general. This section emphasizes the application of MOFs in flexible supercapacitors and flexible batteries.

Most MOFs exhibit poor electrical conductivity due to their bulk electric resistance, which inhibits their rate performance and capacitance performance in energy storage components. Wang et al. carried out a study in which MOF crystals were interweaved with polyaniline (PANI) chains to diminish the system's resistance [70]. The PANI chains were deposited onto the MOF crystals via electrochemical deposition after the Co-based MOF (ZIF-67) crystals were grown on a carbon cloth. The result of this process was a conductive, flexible porous electrode (PANI-ZIF-67-CC) with the underlying MOF's structural framework being left intact. Electrochemical testing results revealed that the electrode presented 2146 mF/cm^2 of areal capacitance at 10 mV/s. This capacitance was much higher than the areal capacitance of an electrode without any PANI deposited onto the MOF crystals (ZIF-67-CC) which had a value of 1.74 mF/cm^2 at 10 mV/s. The ZIF-67 MOF is insulating by nature which explains the comparatively low areal capacitance value. The synergistic effect that occurs following the interweaving of ZIF-67 with PANI facilitates the improved electrochemical properties of the PANI-ZIF-67-CC-based electrode. The PANI chains connect the ZIF-67 crystals thereby becoming bridges for the transportation of electrons to the inner surface of the MOFs improving electronic conduction while the high active surface area of the MOF facilitates high charge storage capacity thereby improving the capacitance. Also, the MOF's porous nature facilitated the generation of a large capacitance as the electrolyte is free to pass through the pores easily. Fig. 17a and b show a schematic representation of this electron conduction process. PANI deposition also leads to a reduction in internal resistance from 4.428 Ω to 3.582 Ω, which was calculated from the Nyquist EIS spectra in Fig. 17d. In addition, the composite electrode exhibits a specific capacitance of 371 F/g at 10 mV/s, based on the CV plots in Fig. 17e. The PANI-ZIF-67-CC electrode was then used to fabricate a flexible, symmetric, solid-state supercapacitor device shown in Fig. 17c. The fabricated supercapacitor exhibited an areal capacitance of 35 mF/cm^2 at a scan rate of 0.05 mA/cm^2 and a stack capacitance of 116 mF/cm^3 at a scan rate of 0.05 mA/cm^2. The supercapacitor also retains more than 80% of its initial capacity following 2000 cycles at 0.1 mA/cm^2.

When it comes to electrode materials suitable for supercapacitors, some carbon-based materials are widely used. This is owing to the low cost of carbon, abundant availability, and excellent chemical stability [69,71]. MOFs have been explored as precursors to obtain 3D hierarchical porous carbon-based materials because of their tunable pore structure and high surface area. This thus makes the resulting MOF-derived carbons exhibit high electric conductivity while also possessing large pore volumes and large surface areas, making them excellent candidates for charge storage, and subsequently delivering high capacitance and power output. Liu et al. synthesized a porous carbon film with

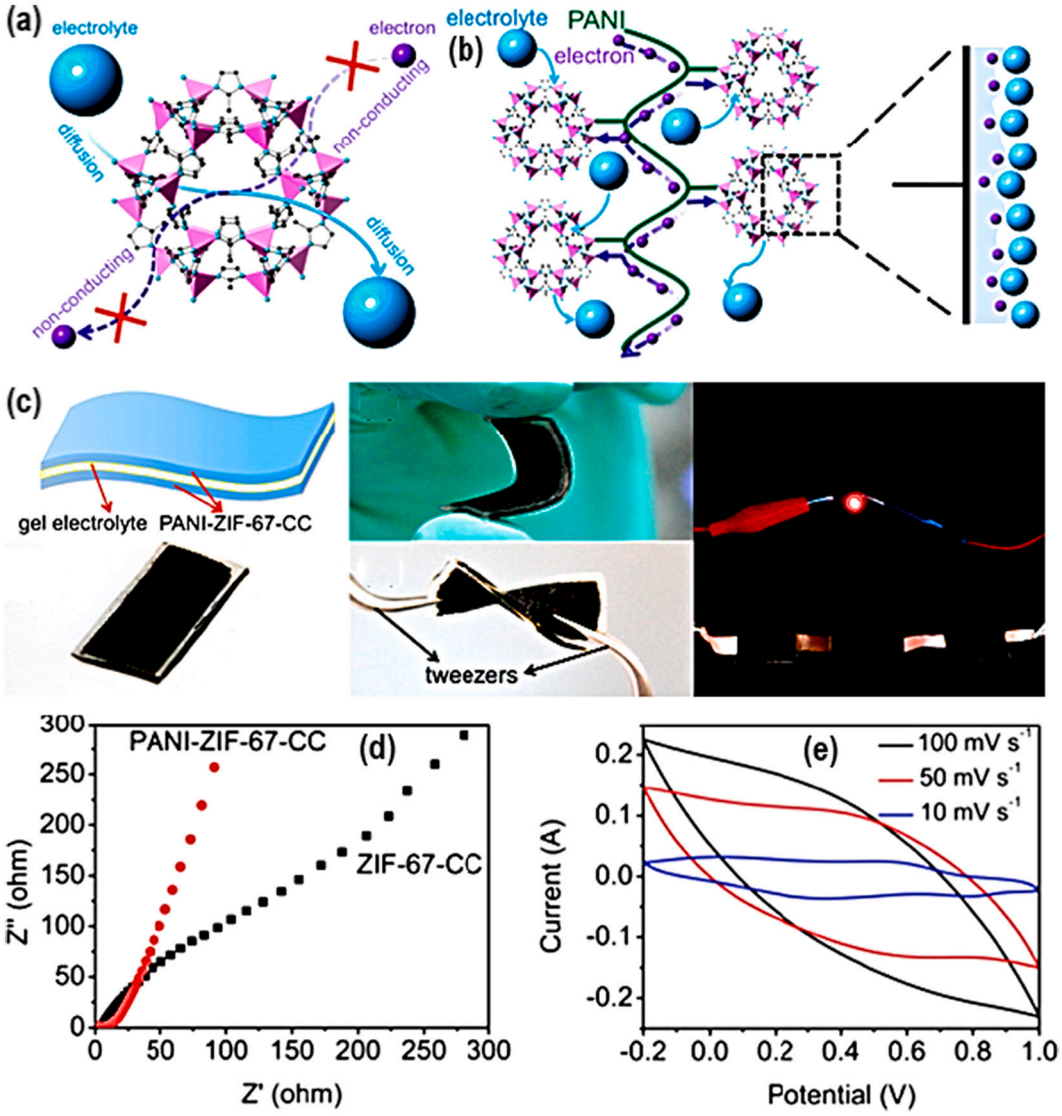

Fig. 17. (a-b) Diagram of electrolyte and electron conduction process in (a) MOF and (b) PANI-interwoven MOF. (c) Schematic diagram showing the flexible solid-state supercapacitor device based on PANI-ZIF-67-CC and photocopies of the supercapacitor devices based on flexible solid-state components under different states namely: neutral, bent, and twisted, demonstrating the device's flexibility. The far-right image shows a red LED that was powered by three supercapacitors connected in series. (d) Nyquist EIS spectra of ZIF-67-CC and PANI-ZIF-67-CC. (e) CV plots for the PANI-ZIF-67-CC at varying scan rates. Adapted with permission [70]. Copyright (2015), American Chemical Society.

appreciable flexibility comprised of MOF-derived porous carbon polyhedrons and CNTs to be used as an electrode material for a flexible, aqueous symmetrical supercapacitor [71]. Electrochemical performance analysis showed that the electrode material exhibited 381.2 F/g of specific capacitance at a scan rate of 5 mV/s and 194.8 F/g at a current density of 2 A/g. Also, a high Coulombic efficiency that was above 95% was obtained along with 10,000 cycles at a current density of 10 A/g thereby showing appreciable cycling stability. The assembled supercapacitor exhibited 157.9 and 128.9 F/g of specific capacitance values at 1 and 10 A/g of current density. The supercapacitor also exhibited a power density of 3500 W/kg at an energy density of around 9.1 Wh/kg. The MOF-derived carbon polyhedrons inherit the porous morphology of the MOF precursor, thereby being a direct cause of the improved electrochemical results which can be assigned to the synergistic effect of the MOF-derived porous carbon polyhedrons and CNT which endows the fabricated electrode with a large specific surface area with a tailored pore structure while also providing excellent flexibility and electrical conductivity without employing the use of any binders.

In another report conducted by Li et al., a $NiCo_2O_4$@Ni-MOF hybrid electrode was fabricated for application in flexible solid-state hybrid supercapacitors [72]. The fabrication followed a facile two-step synthesis approach to obtain arrays of $NiCo_2O_4$ nanowires over carbon cloth, followed by the tailored growth of the Ni-MOF nanoarrays on the $NiCo_2O_4$ nanowires' surface. An illustration of this synthesis process is presented in Fig. 18a, with the morphologies of the pristine $NiCo_2O_4$ nanowires as well as $NiCo_2O_4$@Ni-MOF hybrid nanoarrays presented in Figs. 18b, c, and d. The electrode showed excellent electrochemical performance with 208.8 mAh/g of specific capacity at a current density of 2 mA/cm^2 along with 68.2% of rate capability. Based on the CV plot in Fig. 18e, it could be observed that the $NiCo_2O_4$@Ni-MOF-based electrode demonstrated the largest enclosed CV area and thus demonstrated that the Ni-MOF nanosheets contributed to an increased capacity compared to the other tested electrode materials. This electrode also displays the longest discharge time, as observed in Fig. 18f. The $NiCo_2O_4$@Ni-MOF hybrid electrode was then used as a cathode in the fabrication of a flexible hybrid supercapacitor, while for the anode, activated carbon as employed. The resulting supercapacitor exhibited 32.6 Wh/kg as the maximum energy density at 348.9 W/kg of power

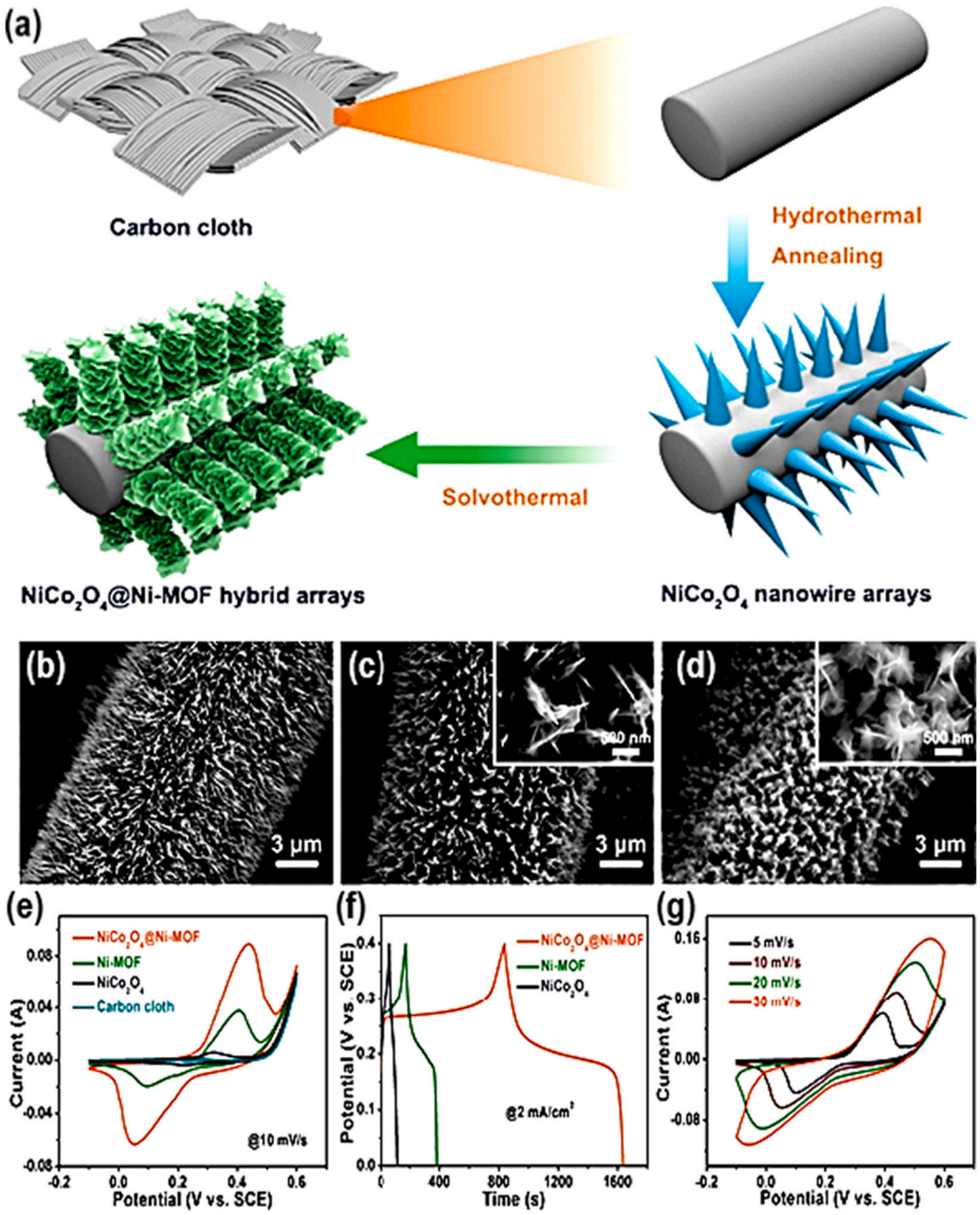

Fig. 18. (a) Scheme displaying the synthesis of $NiCo_2O_4$@Ni-MOF hybrid nanoarrays over carbon cloth via hydrothermal annealing and solvothermal synthesis. (b) SEM micrographs for the neat $NiCo_2O_4$ nanowires over carbon cloth. (c-d) SEM micrographs for the $NiCo_2O_4$@Ni-MOF arrays at varying reaction times. (e) CV plots of $NiCo_2O_4$@Ni-MOF $NiCo_2O_4$, Ni-MOF, carbon cloth, and at 10 mV/s. (f) GCD plots at a current density of 2 mA/cm^2. (g) CV plots of $NiCo_2O_4$@Ni-MOF at varying scan rates. Adapted with permission [72]. Copyright (2019), American Chemical Society.

density while also displaying excellent stability with almost 100% retention following 6000 cycles at a current density of 8 mA/cm^2. Again, we observe synergistic effects, in this case, the synergistic effect of (i) the Ni-MOF providing an appreciable specific surface area as well as rich porosity; and (ii) $NiCo_2O_4$ nanowires improving the electrical conductivity, leading to improved electron transfer kinetics and ionic diffusion in the electrolyte. This, therefore, leads to an overall enhancement of electrochemical performance.

Shifting focus onto the application of MOFs in flexible batteries, Peng et al. prepared Co@ZnO/CNF nanocomposites that were bendable and foldable via a facile electrospinning and annealing process to be employed as an electrode component for flexible Li-ion batteries to be incorporated in wearable electronics [73]. The composites were derived from a ZIF-CoZn MOF precursor. The electrode exhibited superb electrochemical properties, with specific capacity values of 1104.9 mAh/g, 935.6 mAh/g, and 718.1 mAh/g being reported at current densities of 100 mA/g after 150 voltametric cycles, 0.5 A/g, and 1.0 A/g respectively. Capacity fading was found to be negligible after 260 charging and discharging cycles at 2 A/g which is a relatively high current density therefore the electrode is determined to have excellent cycling stability. The notable performance of the device could be attributed to the different morphology brought about by the incorporation of the MOF precursor as well as the bimetallic synergism inherent to the as-prepared Co@ZnO/CNF.

In another study, Zhang et al. grew Co_3O_4/Ni-based MOFs over a carbon cloth as substrate via two-step hydrothermal processes to be used

as an electrode material for a flexible alkaline battery-supercapacitor for hybrid devices [74]. Fig. 19a shows an illustration of the synthetic procedure for this study. This fabricated electrode could be applied directly as an electrode material, that is, without the need for insulating binders or additives to improve conduction as the Co_3O_4 nanowires anchor the MOF onto the carbon cloth. In terms of electrochemical performance, the electrode presented a specific capacity of 209 mAh/g at a current density of 1 A/g while also providing 90% retention suggesting good stability with following 3000 cycles at 1 A/g of current density as shown in the cycling performance curves in Fig. 19e. In addition, Fig. 19b and c show that both electrodes fabricated in this study exhibit an increase in current response with an increase in scanning rate, therefore, suggesting intercalation and deintercalation of hydroxide ions during the electrochemical reaction. GCD analysis reveals that the synthesized composite electrodes display the longest discharge times, as observed in Fig. 19d. This study shows yet another example of the synergistic effect. Incorporation of the Co_3O_4 nanowires promoted an increase in electrical conduction for the overall electrode resulting in improved reaction kinetics while the Ni-MOF's layered structure facilitates favorable intercalation and deintercalation of ions. Additionally, the linker-to-metal-cluster charge-transfer (LCCT) mechanism which exists between the metallic clusters center and the MOF's organic ligands resulted ultimately in excellent capacity performance.

Sharma et al. fabricated a Fe-MOF-based suitable anode for Li-ion batteries that could be used in a flexible battery for electro-thermal heating [75]. The Fe-MOF was configured using two ligands to resolve

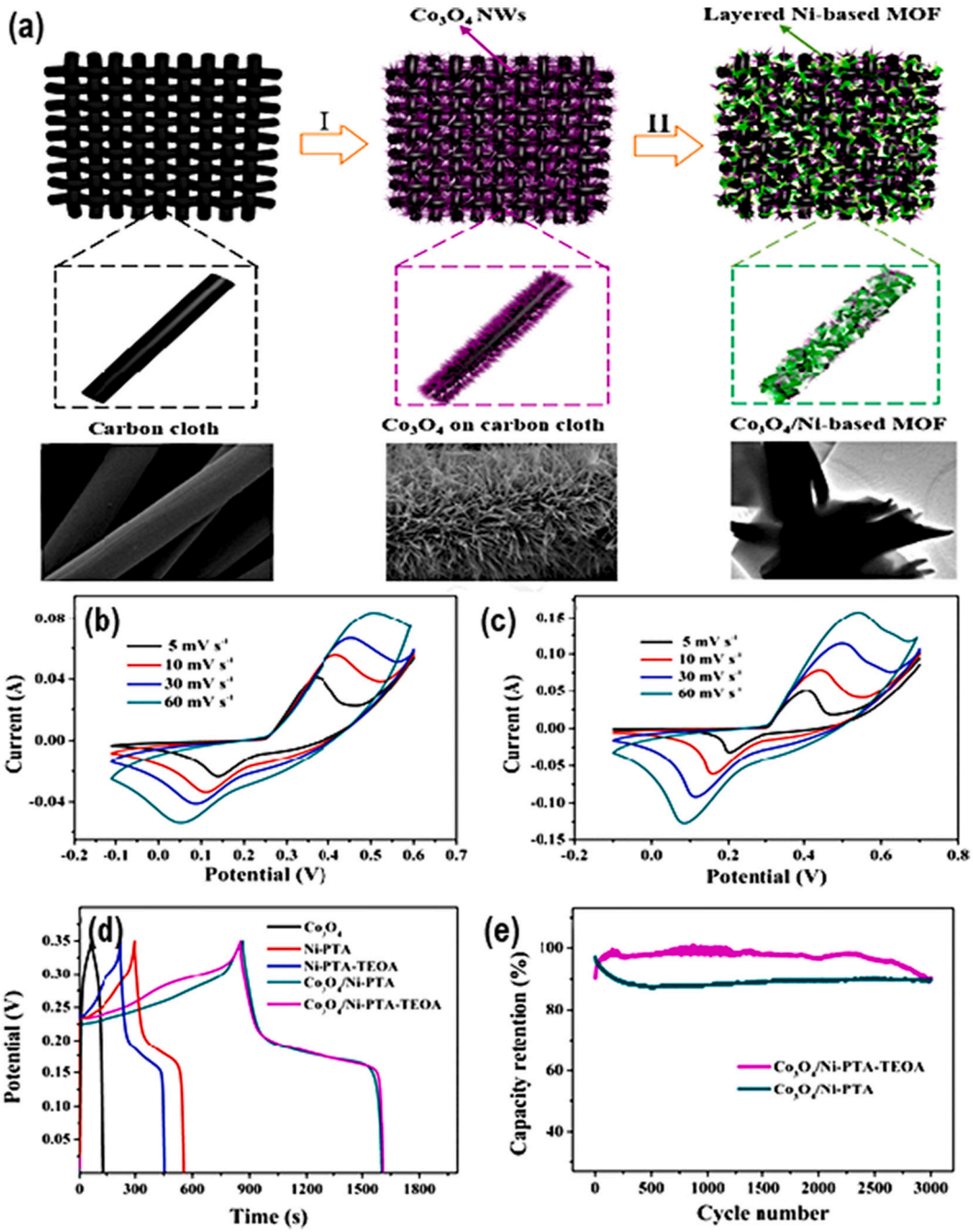

Fig. 19. (a) Diagram showing the synthesis of a MOF based on Co_3O_4/Ni over a carbon cloth via a two-step hydrothermal method. (b) CV plots of Co_3O_4/Ni-PTA electrode at different scan rates. (c) CV plots of Co_3O_4/Ni-PTA-TEOA electrode at varying scan rates. (d) GCD plots of different electroactive materials at a current density of 1 A/g. (e) Cycle performance of Co_3O_4/Ni-PTA and Co_3O_4/Ni-PTA-TEOA electrodes. Adapted with permission [74]. Copyright (2018), Elsevier.

the issue of irreversible capacity loss and rapid capacity decay exhibited by pristine MOFs [75]. As an added advantage, iron is earth-abundant which makes it a promising candidate for the fabrication of MOFs on an industrial scale. The Fe-MOF electrode presented 825 mAh/g of specific capacity at a current density of 250 mA/g after 100 cycles while also exhibiting appreciable cycling stability after 1000 cycles at a current density of 2 A/g. The utilization of a Fe-MOF presenting two ligands along with specific synthesis conditions, in addition to pore tailoring, lead to the formation of dimethylammonium (DMA) cation in situ within the pore. This, therefore, made the resulting MOF present a negligible overall surface area material when the cation was present in the pores, which facilitated the reduction of Li adsorption in the first cycle [75]. Also, the porous nature of the Fe-MOF facilitated the adsorption of a larger number of ions thereby delivering impressive specific capacity values and overall electrochemical properties. The complete device consisted of Fe-MOF and lithium cobalt oxide as the anode and cathode, respectively. The device supplied 360 Wh/kg at a current density of 500 mA/g with excellent stability of 1 k cycles. Table 4 provides a summary of the main results presented in this section.

Table 4
Overview of MOF and MOF-derived components and their electrochemical properties for flexible energy storage device applications compared with other electrocatalysts.

Materials	Application	Specific capacity	Retention (%)	Reference
PANI-ZIF-67-CC	Flexible supercapacitor	371 F/g	80	[70]
HPCF	Flexible supercapacitor	381.2 F/g	95	[71]
$NiCo_2O_4$@Ni-MOF	Flexible supercapacitor	208.8 mAh/g	99	[72]
Co@ZnO/CNF	Flexible battery	935.6 mAh/g	N/A	[73]
Co_3O_4/Ni-PTA	Flexible battery	209 mAh/g	90	[74]
Fe-MOF	Flexible battery	825 mAh/g	N/A	[75]
GeP_3/NbS_2	Flexible battery	540.24 mAh/g	N/A	[76]
MoS_2–SWCNT/CNF	Flexible supercapacitor	605.32 mF/cm	91.01	[77]

4. Conclusion

The design of electrochemical energy storage devices is a pivotal part of the establishment of a clean energy framework. MOFs are a promising group of electroactive components that can be applied in the development of these electrochemical energy storage systems such as batteries and supercapacitors owing to their high specific surface area and their synthetic versatility. The versatility in terms of synthesis of MOFs allows this class of materials to have tunable morphologies and structures, as well as a variety of chemical compositions. This review highlights the various approaches to obtain nanostructured MOFs and summarizes the recent applications of MOFs in supercapacitors (EDLC, pseudocapacitors, and hybrid supercapacitors), batteries (Li-ion, metal-sulfur, and metal-air), and flexible electrochemical energy storage devices (flexible supercapacitors as well as batteries). For the large-scale production of MOFs, the most promising synthesis methods are water-based synthesis methods and solvent-free synthesis methods. Mechanochemical and hydrothermal methods are examples of such synthesis methods with the greatest probability for successful economic and environmental feasibility for large-scale production [20]. As has been presented in this review, we find that the characteristic properties of MOFs (synthetic tunability, porosity, appreciable surface area, etc.) are what facilitate the improved electrochemical properties of these devices and are the key to the future advancement of electrochemical storage devices.

The advancement of electrochemical energy storage devices is largely driven by the discovery and application of novel materials. The future development of MOFs is key to addressing several challenges facing leading electrochemical energy storage device technologies. The introduction of solid-state electrolytes is an area in which MOFs can be applied due to excellent ion mobility resulting from soft chemical interactions, as well as favorable compatibility with carbon-based electrodes [78]. Additionally, the development of MOF solid-electrolyte interfaces (SEI) for batteries is an encouraging future direction for the application of MOFs as MOF SEIs are more accommodating to volumetric changes due to cycling and thus the resulting SEI is less prone to cycling damages [78].

However, even with the great progress that has been achieved in MOF research in recent years, MOF-based energy storage systems are still limited to academic research and not commercially produced. Poor electrical conductivity inherent to MOFs is a major reason inhibiting their commercial production and as such current research is devoted to solving this issue through various means. As has been highlighted in this review, these means include: (i) developing MOFs with different morphologies/structures that enhance conductivity such as layered nanostructured MOFs, and (ii) incorporating conductive additives into the MOF structure such as CNTs, graphene, and conducting polymers such as PANI. These methods not only enhance the electrical conductivity of the MOFs but also contribute to increasing the already high specific surface areas inherent to the MOF structure. Other reasons inhibiting the commercial production of MOFs include: (i) Stability concerns whereby the MOF structure is susceptible to collapse even under mild conditions due to weak coordinated bonds between the metallic centers and the organic group; and (ii) fabrication and characterization of MOFs is still costly, owing to expensive characterization equipment and starting materials [17]. The main solution to these issues, we find, is by further developing methods to efficiently obtain MOF-based materials. Synthetical approaches such as electrochemical, mechanochemical, and microwave syntheses were developed specifically to address these challenges to reduce the complexity of the large-scale MOF synthesis process [20]. By reducing the synthesis complexity, overall synthesis costs can decrease thereby making the large-scale production of MOFs more economically viable.

All in all, the incorporation of MOFs into electrochemical energy storage devices does lead to improved electrochemical performance, and with their diverse chemical compositions and tunable structures, researchers can conduct a wide range of studies on these materials. The result of these research efforts, we expect, will therefore be the further development and improvement of MOFs' electrochemical performance, culminating in the scalability of MOF-based energy systems.

Declaration of Competing Interest

The authors declare that they have no known competing financial interests.

Data availability

No data was used for the research described in the article.

References

[1] J. Rehman, K. Eid, R. Ali, X. Fan, G. Murtaza, M. Faizan, A. Laref, W. Zheng, R. S. Varma, Engineering of transition metal sulfide nanostructures as efficient electrodes for high-performance supercapacitors, ACS Appl. Energy Mater. 5 (2022) 6481–6498.
[2] Q. Peng, J. Rehman, K. Eid, A.S. Alofi, A. Laref, M.D. Albaqami, R.G. Alotabi, M. F. Shibl, Vanadium carbide (V4C3) MXene as an efficient anode for Li-Ion and Na-Ion batteries, Nanomaterials. 12 (2022).
[3] Y. Ibrahim, A. Mohamed, A.M. Abdelgawad, K. Eid, A.M. Abdullah, A. Elzatahry, The recent advances in the Mechanical properties of self-standing two-dimensional MXene-based nanostructures: deep insights into the supercapacitor, Nanomaterials. 10 (2020).
[4] A.K. Ipadeola, A.B. Haruna, L. Gaolatlhe, A.K. Lebechi, J. Meng, Q. Pang, K. Eid, A. M. Abdullah, K.I. Ozoemena, Efforts at enhancing bifunctional electrocatalysis and related events for rechargeable zinc-air batteries, ChemElectroChem. 8 (2021) 3998–4018.

[5] H. Wang, S. Yin, K. Eid, Y. Li, Y. Xu, X. Li, H. Xue, L. Wang, Fabrication of mesoporous cage-bell Pt nanoarchitectonics as efficient catalyst for oxygen reduction reaction, ACS Sustain. Chem. Eng. 6 (2018) 11768–11774.
[6] A.K. Lebechi, A.K. Ipadeola, K. Eid, A.M. Abdullah, K.I. Ozoemena, Porous spinel-type transition metal oxide nanostructures as emergent electrocatalysts for oxygen reduction reactions, Nanoscale. 14 (2022) 10717–10737.
[7] G. Xu, P. Nie, H. Dou, B. Ding, L. Li, X. Zhang, Exploring metal organic frameworks for energy storage in batteries and supercapacitors, Mater. Today 20 (2017) 191–209.
[8] O.M. Yaghi, G. Li, H. Li, Selective binding and removal of guests in a microporous metal–organic framework, Nature. 378 (1995) 703–706.
[9] J. Choi, T. Ingsel, D. Neupane, S.R. Mishra, A. Kumar, R.K. Gupta, Metal-organic framework-derived cobalt oxide and sulfide having nanoflowers architecture for efficient energy conversion and storage, J. Energy Storage. 50 (2022), 104145.
[10] M. Barona, R.Q. Snurr, Exploring the tunability of trimetallic MOF nodes for partial oxidation of methane to methanol, ACS Appl. Mater. Interfaces 12 (2020) 28217–28231.
[11] X.F. Lu, Y. Fang, D. Luan, X.W.D. Lou, Metal–organic frameworks derived functional materials for electrochemical energy storage and conversion: a mini review, Nano Lett. 21 (2021) 1555–1565.
[12] Z. Song, L. Zhang, M. Zheng, X. Sun, Chapter 1 MOF-derived materials for extremely efficient electrocatalysis, in: Layer. Mater. Energy Storage Convers., The Royal Society of Chemistry, 2019, pp. 1–38.
[13] R.R. Salunkhe, Y.V. Kaneti, Y. Yamauchi, Metal–organic framework-derived nanoporous metal oxides toward supercapacitor applications: progress and prospects, ACS Nano 11 (2017) 5293–5308.
[14] H. Wang, Q.-L. Zhu, R. Zou, Q. Xu, Metal-organic frameworks for energy applications, Chem. 2 (2017) 52–80.
[15] B. Xu, H. Zhang, H. Mei, D. Sun, Recent progress in metal-organic framework-based supercapacitor electrode materials, Coord. Chem. Rev. 420 (2020), 213438.
[16] B. He, Q. Zhang, Z. Pan, L. Li, C. Li, Y. Ling, Z. Wang, M. Chen, Z. Wang, Y. Yao, Q. Li, L. Sun, J. Wang, L. Wei, Freestanding metal–organic frameworks and their derivatives: an emerging platform for electrochemical energy storage and conversion, Chem. Rev. 122 (2022) 10087–10125.
[17] S. Tajik, H. Beitollahi, F.G. Nejad, K.O. Kirlikovali, Q. Van Le, H.W. Jang, R. S. Varma, O.K. Farha, M. Shokouhimehr, Recent electrochemical applications of metal–organic framework-based materials, Cryst. Growth Des. 20 (2020) 7034–7064.
[18] T. Qiu, Z. Liang, W. Guo, H. Tabassum, S. Gao, R. Zou, Metal–organic framework-based materials for energy conversion and storage, ACS Energy Lett. 5 (2020) 520–532.
[19] W.H. Bin, L.X.W. David, Metal-organic frameworks and their derived materials for electrochemical energy storage and conversion: promises and challenges, Sci. Adv. 3 (2022) eaap9252.
[20] M. Rubio-Martinez, C. Avci-Camur, A.W. Thornton, I. Imaz, D. Maspoch, M.R. Hill, New synthetic routes towards MOF production at scale, Chem. Soc. Rev. 46 (2017) 3453–3480.
[21] N. Stock, S. Biswas, Synthesis of metal-organic frameworks (MOFs): routes to various MOF topologies, morphologies, and composites, Chem. Rev. 112 (2012) 933–969.
[22] 4 - Phosphor-converted LEDs, in: G.B. Nair, S.J. Dhoble, G.B. Nair, S.J.B.T.-T.F. and A, L.-E.D. Dhoble (Eds.), Woodhead Publ. Ser. Electron. Opt. Mater., Woodhead Publishing, 2021, pp. 87–126.
[23] A.K. Gupta, M. Saraf, P.K. Bharadwaj, S.M. Mobin, Dual functionalized CuMOF-based composite for high-performance supercapacitors, Inorg. Chem. 58 (2019) 9844–9854.
[24] Y. Zhao, Z. Song, X. Li, Q. Sun, N. Cheng, S. Lawes, X. Sun, Metal organic frameworks for energy storage and conversion, Energy Storage Mater. 2 (2016) 35–62.
[25] C. Vaitsis, G. Sourkouni, C. Argirusis, Metal Organic Frameworks (MOFs) and ultrasound: a review, Ultrason. Sonochem. 52 (2019) 106–119.
[26] J. Beamish-Cook, K. Shankland, C.A. Murray, P. Vaqueiro, Insights into the mechanochemical synthesis of MOF-74, Cryst. Growth Des. 21 (2021) 3047–3055.
[27] M. Klimakow, P. Klobes, A.F. Thünemann, K. Rademann, F. Emmerling, Mechanochemical synthesis of metal−organic frameworks: a fast and facile approach toward quantitative yields and high specific surface areas, Chem. Mater. 22 (2010) 5216–5221.
[28] T. Tsuzuki, Mechanochemical synthesis of metal oxide nanoparticles, Commun. Chem. 4 (2021) 143.
[29] R.F. Mendes, J. Rocha, F.A. Almeida Paz, Chapter 8 - Microwave synthesis of metal-organic frameworks, in: B.A. Mozafari (Ed.), M.B.T.-M.-O.F, Woodhead Publishing, 2020, pp. 159–176.
[30] C. Chen, X. Feng, Q. Zhu, R. Dong, R. Yang, Y. Cheng, C. He, Microwave-assisted rapid synthesis of well-shaped MOF-74 (Ni) for CO2 efficient capture, Inorg. Chem. 58 (2019) 2717–2728.
[31] V. M. V, G. Nageswaran, Review—direct electrochemical synthesis of metal organic frameworks, J. Electrochem. Soc. 167 (2020), 155527.
[32] Y. Wang, Y. Liu, H. Wang, W. Liu, Y. Li, J. Zhang, H. Hou, J. Yang, Ultrathin NiCo-MOF nanosheets for high-performance supercapacitor electrodes, ACS Appl. Energy Mater. 2 (2019) 2063–2071.
[33] T.P. Sumangala, M.S. Sreekanth, A. Rahaman, Applications of supercapacitors BT - Handbook of nanocomposite supercapacitor materials III: selection, in: K.K. Kar (Ed.), Springer International Publishing, Cham, 2021, pp. 367–393.
[34] X. Chen, R. Paul, L. Dai, Carbon-based supercapacitors for efficient energy storage, Natl. Sci. Rev. 4 (2017) 1–37.
[35] M. Tomy, A. Ambika Rajappan, V. VM, X. Thankappan Suryabai, Emergence of novel 2D materials for high-performance supercapacitor electrode applications: a brief review, Energy Fuel 35 (2021) 19881–19900.
[36] Y. Wang, J. Zhou, K. Chen, W. Zhao, K. Tao, L. Han, Metal–organic framework-derived Bi2O3/C and NiCo2S4 hollow nanofibers for asymmetric supercapacitors, ACS Appl. Nano Mater. 4 (2021) 11895–11906.
[37] Y. Li, H. Xie, J. Li, Y. Yamauchi, J. Henzie, Metal–organic framework-derived CoOx/carbon composite array for high-performance supercapacitors, ACS Appl. Mater. Interfaces 13 (2021) 41649–41656.
[38] X. Xu, J. Yang, Y. Hong, J. Wang, Nitrate precursor driven high performance Ni/Co-MOF nanosheets for supercapacitors, ACS Appl. Nano Mater. 5 (2022) 8382–8392.
[39] J. Yang, P. Xiong, C. Zheng, H. Qiu, M. Wei, Metal–organic frameworks: a new promising class of materials for a high performance supercapacitor electrode, J. Mater. Chem. A 2 (2014) 16640–16644.
[40] Y. Zhou, Z. Mao, W. Wang, Z. Yang, X. Liu, In-situ fabrication of graphene oxide hybrid Ni-based metal–organic framework (Ni–MOFs@GO) with ultrahigh capacitance as electrochemical pseudocapacitor materials, ACS Appl. Mater. Interfaces 8 (2016) 28904–28916.
[41] Q. Wang, Q. Wang, B. Xu, F. Gao, F. Gao, C. Zhao, Flower-shaped multiwalled carbon nanotubes@nickel-trimesic acid MOF composite as a high-performance cathode material for energy storage, Electrochim. Acta 281 (2018) 69–77.
[42] O. Sadak, W. Wang, J. Guan, A.K. Sundramoorthy, S. Gunasekaran, MnO2 nanoflowers deposited on graphene paper as electrode materials for supercapacitors, ACS Appl. Nano Mater. 2 (2019) 4386–4394.
[43] J.-L. Yi, X.-H. Yu, R.-L. Zhang, L. Liu, Chitosan-based synthesis of O, N, and P codoped hierarchical porous carbon as electrode materials for supercapacitors, Energy Fuel 35 (2021) 20339–20348.
[44] K.M. Choi, H.M. Jeong, J.H. Park, Y.-B. Zhang, J.K. Kang, O.M. Yaghi, Supercapacitors of nanocrystalline metal–organic frameworks, ACS Nano 8 (2014) 7451–7457.
[45] H. Qiao, Q. Wei, 10 - Functional nanofibers in lithium-ion batteries, in: Q.B.T.-F.N, A. Wei (Eds.), Woodhead Publ. Ser. Text, Woodhead Publishing, 2012, pp. 197–208.
[46] F.-B. Wu, B. Yang, J.-L.B.T.-G.E.S.S, in: A. Ye (Ed.), Chapter 2 - Technologies of Energy Storage Systems, Academic Press, 2019, pp. 17–56.
[47] C. Wang, Y. Yu, J. Niu, Y. Liu, D. Bridges, X. Liu, J. Pooran, Y. Zhang, A. Hu, Recent Progress of Metal–Air Batteries—A Mini Review, Appl. Sci. 9 (2019).
[48] Q. Liu, Z. Pan, E. Wang, L. An, G. Sun, Aqueous metal-air batteries: fundamentals and applications, Energy Storage Mater. 27 (2020) 478–505.
[49] S. Maiti, A. Pramanik, U. Manju, S. Mahanty, Reversible lithium storage in manganese 1,3,5-Benzenetricarboxylate metal–organic framework with high capacity and rate performance, ACS Appl. Mater. Interfaces 7 (2015) 16357–16363.
[50] Y. Jin, C. Zhao, Z. Sun, Y. Lin, L. Chen, D. Wang, C. Shen, Facile synthesis of Fe-MOF/RGO and its application as a high performance anode in lithium-ion batteries, RSC Adv. 6 (2016) 30763–30768.
[51] T. Li, Y. Tong, J. Li, Z. Kong, X. Liu, H. Xu, K. Wang, H. Jin, Hericium erinaceus-like copper-based MOFs as anodes for high performance lithium ion batteries, ACS Appl. Energy Mater. 4 (2021) 11400–11407.
[52] P.M. Shanthi, P.J. Hanumantha, B. Gattu, M. Sweeney, M.K. Datta, P.N. Kumta, Understanding the origin of irreversible capacity loss in non-carbonized carbonate − based metal organic framework (MOF) Sulfur hosts for Lithium − Sulfur battery, Electrochim. Acta 229 (2017) 208–218.
[53] G. Xu, Y. Zuo, B. Huang, Metal-organic framework-74-Ni/carbon nanotube composite as sulfur host for high performance lithium-sulfur batteries, J. Electroanal. Chem. 830–831 (2018) 43–49.
[54] Z. Wu, H. Wu, T. Niu, S. Wang, G. Fu, W. Jin, T. Ma, Sulfurated metal–organic framework-derived nanocomposites for efficient bifunctional oxygen electrocatalysis and rechargeable Zn–Air battery, ACS Sustain. Chem. Eng. 8 (2020) 9226–9234.
[55] Y.-W. Li, W.-J. Zhang, J. Li, H.-Y. Ma, H.-M. Du, D.-C. Li, S.-N. Wang, J.-S. Zhao, J.-M. Dou, L. Xu, Fe-MOF-derived efficient ORR/OER bifunctional electrocatalyst for rechargeable zinc–air batteries, ACS Appl. Mater. Interfaces 12 (2020) 44710–44719.
[56] H. Liu, L. Zhao, Y. Xing, J. Lai, L. Li, F. Wu, N. Chen, R. Chen, Enhancing the long cycle performance of Li–O2 batteries at high temperatures using metal–organic framework-based electrolytes, ACS Appl. Energy Mater. 5 (2022) 7185–7191.
[57] T.-E. Fan, X. Tang, S.-M. Liu, CuFeS2 nanosheets assembled into honeycomb-like microspheres as stable high-capacity anodes for sodium-ion batteries, ACS Appl. Nano Mater. 5 (2022) 10392–10398.
[58] L. Li, S. Liao, G. Dong, K. Jiang, Y. Liu, C. Zhang, J. Yan, K. Ye, J. Yao, G. Wang, K. Zhu, D. Cao, V2O3 nanoparticles anchored on an interconnected carbon nanosheet network toward high-performance sodium-ion batteries, ACS Appl. Energy Mater. 5 (2022) 12707–12715.
[59] D. Li, D. Yan, X. Zhang, J. Li, T. Lu, L. Pan, Porous CuO/reduced graphene oxide composites synthesized from metal-organic frameworks as anodes for high-performance sodium-ion batteries, J. Colloid Interface Sci. 497 (2017) 350–358.
[60] B. Ramaraju, C.-H. Li, S. Prakash, C.-C. Chen, Metal–organic framework derived hollow polyhedron metal oxide posited graphene oxide for energy storage applications, Chem. Commun. 52 (2016) 946–949.
[61] A. Tang, X. He, H. Yin, Y. Li, Y. Zhang, S. Huang, D.G. Truhlar, UiO-66 metal–organic framework as an anode for a potassium-ion battery: quantum mechanical analysis, J. Phys. Chem. C 125 (2021) 9679–9687.
[62] Y. Zuo, P. Li, R. Zang, S. Wang, Z. Man, P. Li, S. Wang, W. Zhou, Sulfur-Doped flowerlike porous carbon derived from metal–organic frameworks as a high-

performance potassium-ion battery anode, ACS Appl. Energy Mater. 4 (2021) 2282–2291.
[63] J. Shin, M. Kim, J. Cirera, S. Chen, G.J. Halder, T.A. Yersak, F. Paesani, S.M. Cohen, Y.S. Meng, MIL-101(Fe) as a lithium-ion battery electrode material: a relaxation and intercalation mechanism during lithium insertion, J. Mater. Chem. A 3 (2015) 4738–4744.
[64] F. Keshavarz, M. Kadek, B. Barbiellini, A. Bansil, Electrochemical potential of the metal organic framework MIL-101(Fe) as cathode material in Li-Ion batteries, Condens. Matter 6 (2021) 22.
[65] J.L. Mancuso, A.M. Mroz, K.N. Le, C.H. Hendon, Electronic structure modeling of metal–organic frameworks, Chem. Rev. 120 (2020) 8641–8715.
[66] K. Trepte, S. Schwalbe, G. Seifert, Electronic and magnetic properties of DUT-8(Ni), Phys. Chem. Chem. Phys. 17 (2015) 17122–17129.
[67] T. Yamada, K. Shiraishi, H. Kitagawa, N. Kimizuka, Applicability of MIL-101(Fe) as a cathode of lithium ion batteries, Chem. Commun. 53 (2017) 8215–8218.
[68] L. Lin, H. Ning, S. Song, C. Xu, N. Hu, Flexible electrochemical energy storage: the role of composite materials, Compos. Sci. Technol. 192 (2020), 108102.
[69] J. Cherusseri, D. Pandey, K. Sambath Kumar, J. Thomas, L. Zhai, Flexible supercapacitor electrodes using metal–organic frameworks, Nanoscale. 12 (2020) 17649–17662.
[70] L. Wang, X. Feng, L. Ren, Q. Piao, J. Zhong, Y. Wang, H. Li, Y. Chen, B. Wang, Flexible solid-state supercapacitor based on a metal–organic framework interwoven by electrochemically-deposited PANI, J. Am. Chem. Soc. 137 (2015) 4920–4923.
[71] Y. Liu, G. Li, Y. Guo, Y. Ying, X. Peng, Flexible and binder-free hierarchical porous carbon film for supercapacitor electrodes derived from MOFs/CNT, ACS Appl. Mater. Interfaces 9 (2017) 14043–14050.
[72] G. Li, H. Cai, X. Li, J. Zhang, D. Zhang, Y. Yang, J. Xiong, Construction of hierarchical NiCo2O4@Ni-MOF hybrid arrays on carbon cloth as superior battery-type electrodes for flexible solid-state hybrid supercapacitors, ACS Appl. Mater. Interfaces 11 (2019) 37675–37684.
[73] J. Peng, J. Tao, Z. Liu, Y. Yang, L. Yu, M. Zhang, F. Wang, Y. Ding, Ultra-stable and high capacity flexible lithium-ion batteries based on bimetallic MOFs derivatives aiming for wearable electronic devices, Chem. Eng. J. 417 (2021), 129200.
[74] L. Zhang, Y. Zhang, S. Huang, Y. Yuan, H. Li, Z. Jin, J. Wu, Q. Liao, L. Hu, J. Lu, S. Ruan, Y.-J. Zeng, Co3O4/Ni-based MOFs on carbon cloth for flexible alkaline battery-supercapacitor hybrid devices and near-infrared photocatalytic hydrogen evolution, Electrochim. Acta 281 (2018) 189–197.
[75] N. Sharma, S. Szunerits, R. Boukherroub, R. Ye, S. Melinte, M.O. Thotiyl, S. Ogale, Dual-Ligand Fe-Metal organic framework based robust high capacity Li Ion battery anode and its use in a flexible battery format for electro-thermal heating, ACS Appl. Energy Mater. 2 (2019) 4450–4457.
[76] J. Liu, Y. Liu, Y. Yang, X. Bai, L. Liu, K. Yang, H. Ali, Y. Zhao, B. Wu, B. Sa, C. Wen, Q. Peng, Z. Sun, GeP3/NbX2 (X=S, Se) nano-heterostructures: promising isotropic flexible anodes for lithium-ion batteries with high lithium storage capacity, ACS Omega. 6 (2021) 2956–2965.
[77] H. Chang, L. Zhang, S. Lyu, S. Wang, Flexible and freestanding MoS2 Nanosheet/Carbon Nanotube/Cellulose nanofibril hybrid aerogel film for high-performance all-solid-state supercapacitors, ACS Omega. 7 (2022) 14390–14399.
[78] A.E. Baumann, D.A. Burns, B. Liu, V.S. Thoi, Metal-organic framework functionalization and design strategies for advanced electrochemical energy storage devices, Commun. Chem. 2 (2019) 86.